ALMA MATER STUDIORUM
UNIVERSITÀ DI BOLOGNA

Fifth workshop on millimeter astronomy in Bologna

INAF
ISTITUTO NAZIONALE
DI ASTROFISICA

Probing the gas reservoirs of high-z dusty galaxies using ALMA observations of atomic carbon

Gayathri GURURAJAN,

Matthieu Béthermin, Justin Spilker, Patrice Theulé and
the SPT-SMG collaboration

Dusty star-forming galaxies

- A population of massive galaxies (> 10^{11} $M_\odot$, e.g., Reichers+13) with prodigious star-formation rates (> 500 $M_\odot$/yr).
- Suspected : A combination of a large reservoir and boosted star formation efficiencies (Harris+12, Ivison+12, Tan+14, Aravena+16, Ciesla+20, Jarugula+21).
- Characterising the gas reservoirs : understanding the nature and evolution of intensely star-forming dusty galaxies.
- Direct observations of H_2 not feasible – thus we use *tracers.*
- Tracers such as CO, [CI], dust, and [CII] can be used to estimate the molecular gas content of a galaxy.

Credits : Daddi et al., 2010b

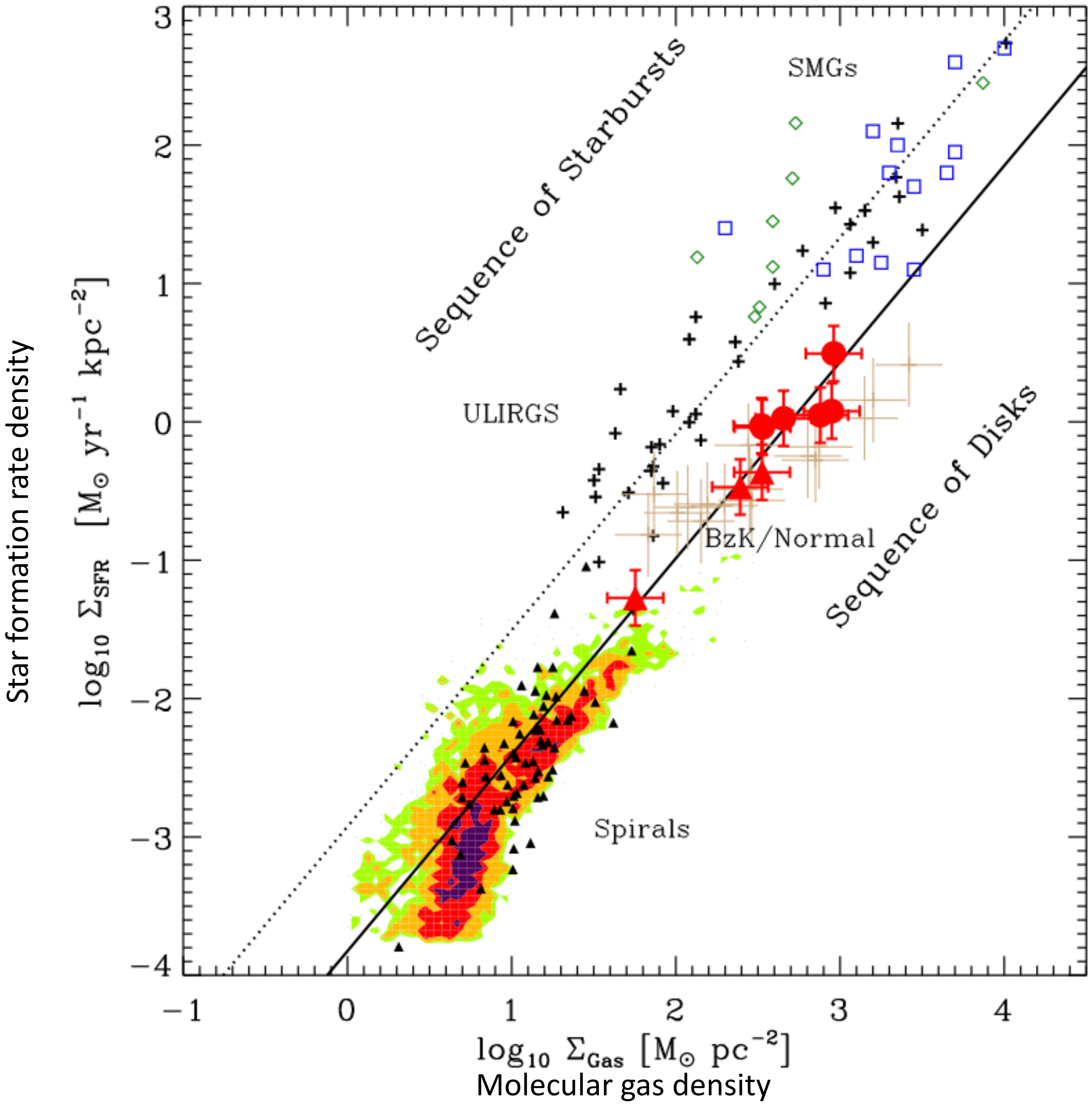

Molecular Gas mass estimators/tracers

CO molecule

- To assume : $\boldsymbol{\alpha}_{CO}$
- Excitation to obtain CO(1-0) flux from other CO transitions

$$M(H_2)^{CO} = \alpha_{CO} L'_{CO(1-0)} \; [M_\odot],$$

Neutral carbon lines - [CI]

- To assume : X_{CI}
- Q_{10} can be computed if both the [CI] transitions can be observed

$$M(H_2)^{[CI]} = 3.39 \times 10^{-2} \frac{L_{[CI]}}{\underline{Q_{10}} X_{CI}} \; [M_\odot],$$

Ionised carbon fine structure line - [CII]

- To assume : $\boldsymbol{\alpha}_{[CII]}$

$$M(H_2)^{[CII]} = \alpha_{[CII]} L_{[CII]} \; [M_\odot],$$

Dust

- To assume : $\boldsymbol{\delta}_{GDR}$
- Estimation of dust mass based on SED fitting

$$M(H_2)^{dust} = \delta_{GDR} M_{dust} \; [M_\odot],$$

Questions

1. How efficient are [CI] emission lines as a tracer of the molecular gas content?
2. Can we cross-calibrate different tracers to see if they can agree with one another?

Gravitationally lensed DSFGs

- Lensing preserves surface brightness.
- Stretches the source – Boosts apparent total flux, thus enabling the detection of faint sources.
- Integration time for an unresolved source $\propto \mu^{-2}$ thus saving precious telescope time!
- Resolved sources/high-resolution observations : Increases the apparent source size, thus revealing smaller details (even to sub-kpc scales).

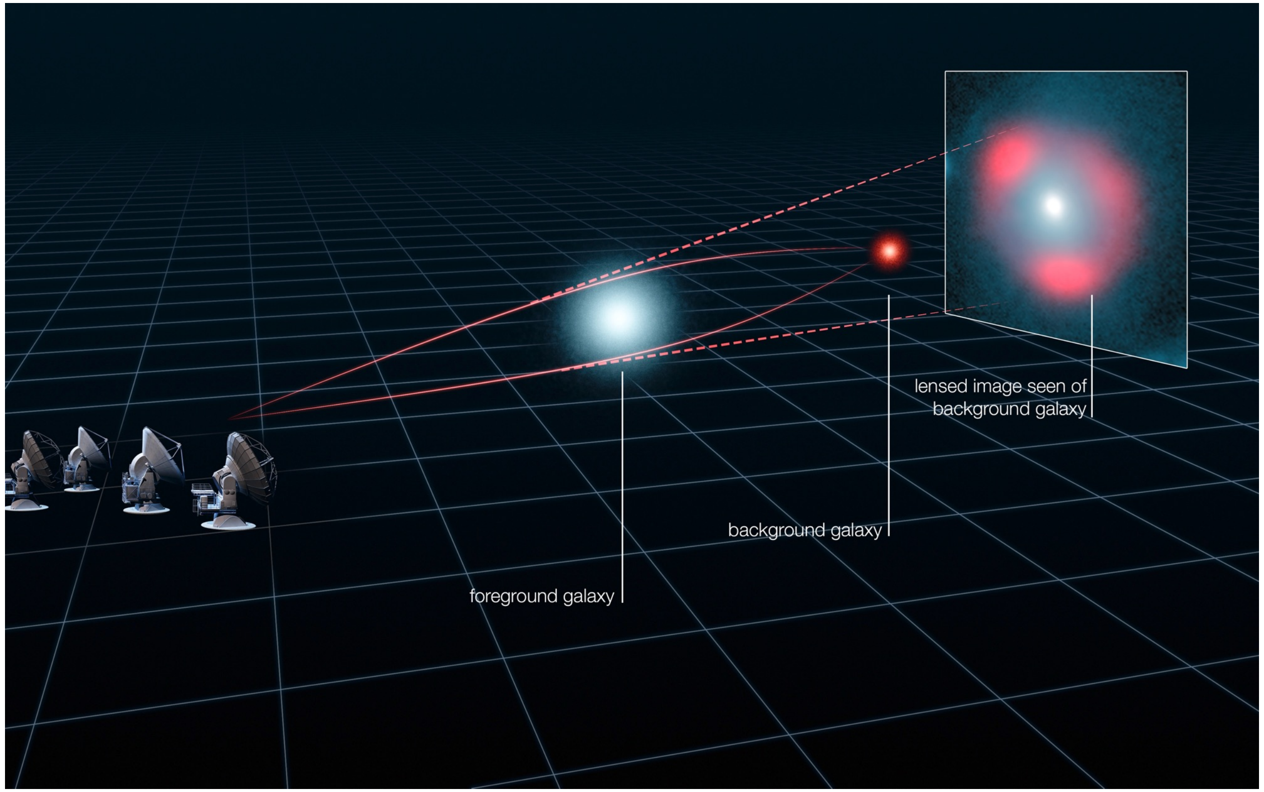

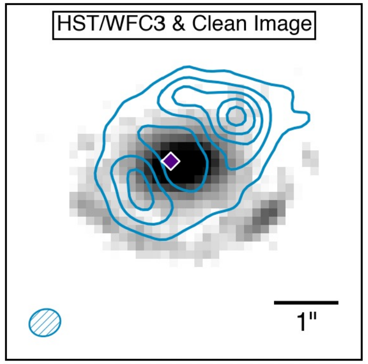

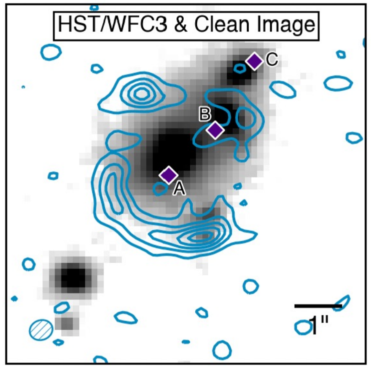

Credits : Left: SPT-SMG collaboration (Vieira et al. 2013; Weiss et al. 2013), Right : Spilker et al. 2016.

Questions

1. How efficient are [CI] emission lines as a tracer of the molecular gas content?
2. Can we cross-calibrate different tracers to see if they can agree with one another?
3. What insights can high-resolution spectral imaging give us on the nature of these objects?
4. What are the effects of differential magnification on these galaxies?

Observations of neutral carbon in 29 high-z lensed dusty star forming galaxies and the comparison of gas mass tracers

Gururajan+23
accepted to A&A, arXiv:2306.03153

Sample

- Target : SPT-SMGs with both [CI] transitions in the observable windows of ALMA.

- Ancillary data : [CII], low-J and mid-J CO lines and dust mass estimations (Gullberg+14, Aravena+16, Bothwell+17, Reuter+20).

- Lines observed with ACA : [CI](1-0), [CI](2-1), CO(7-6) and CO(4-3) for a few sources. Lines observed with APEX : [CII].

- Final sample : 29 SPT-SMGs in redshift range 1.8 – 4.7

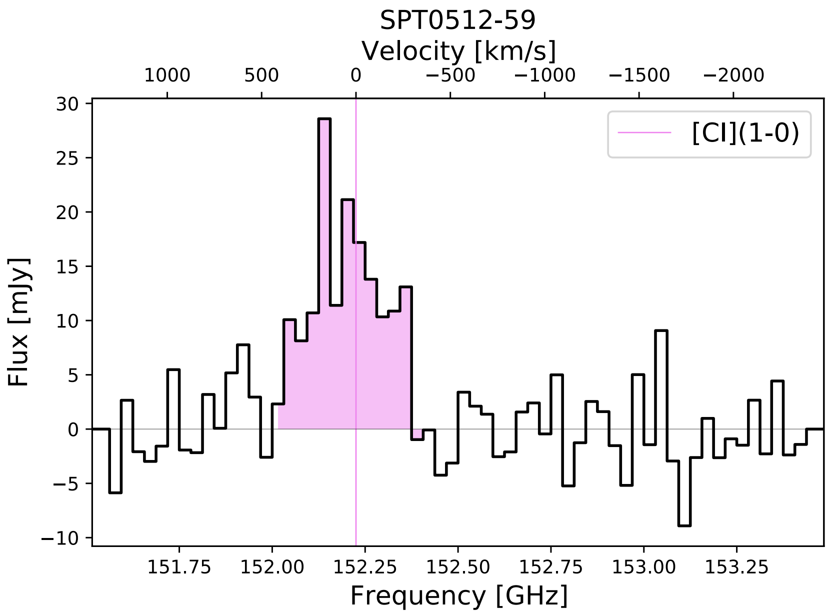

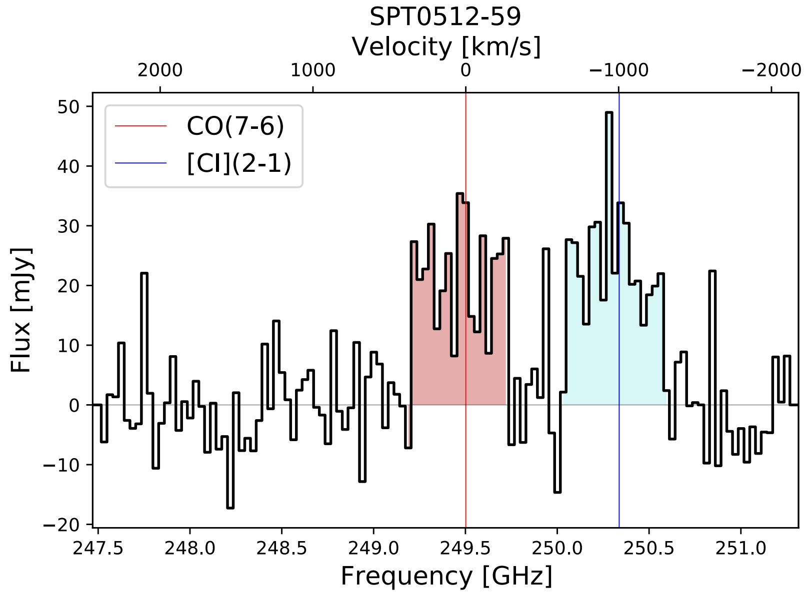

ISM properties with line ratios

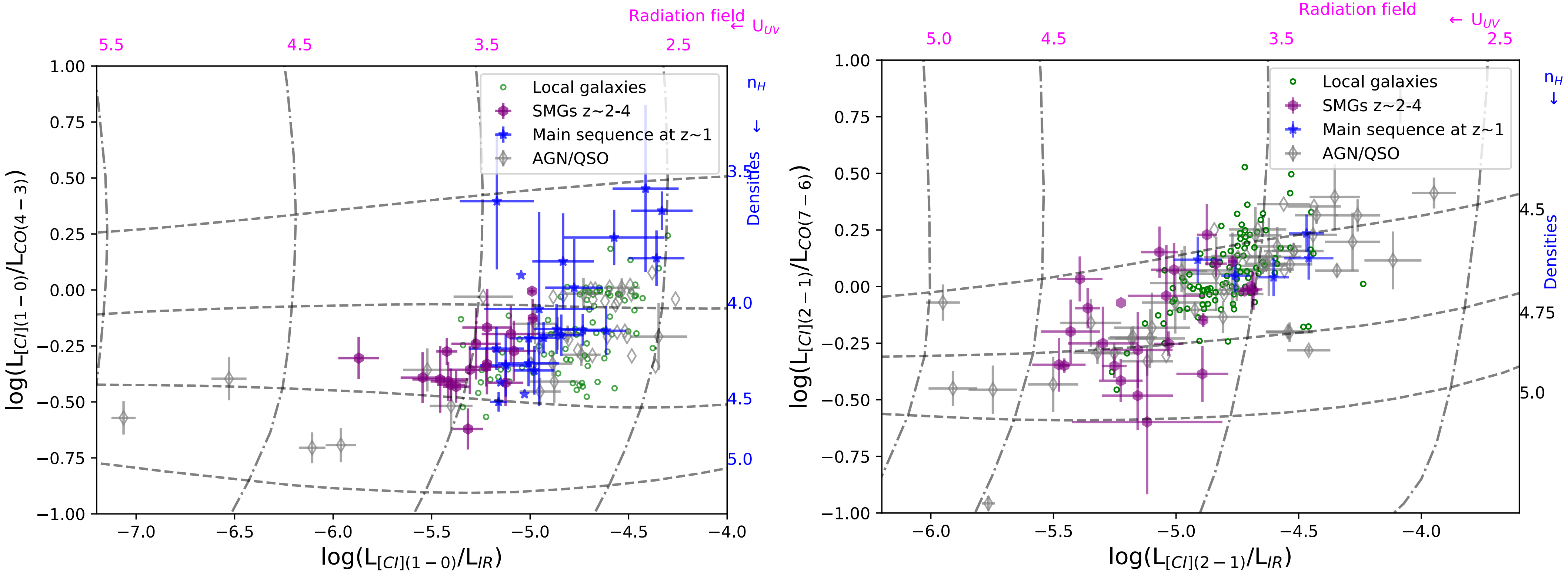

- $L_{[CI](2\text{-}1)}/L_{CO(7\text{-}6)}$ and $L_{[CI](1\text{-}0)}/L_{CO(4\text{-}3)}$: extended versus dense gas tracer (proxy of the density).

- $L_{[CI](2\text{-}1)}/L_{IR}$ and $L_{[CI](1\text{-}0)}/L_{IR}$: total gas content versus star-formation (proxy of the star-formation efficiency).

Valentino+20 sample

Walter et al. 2011; Alaghband-Zadeh et al. 2013; Bothwell et al. 2017; Yang et al. 2017; Andreani et al. 2018; Cañameras et al. 2018; Nesvadba et al. 2018; Dannerbauer et al. 2019; Jin et al. 2019

ISM properties with line ratios

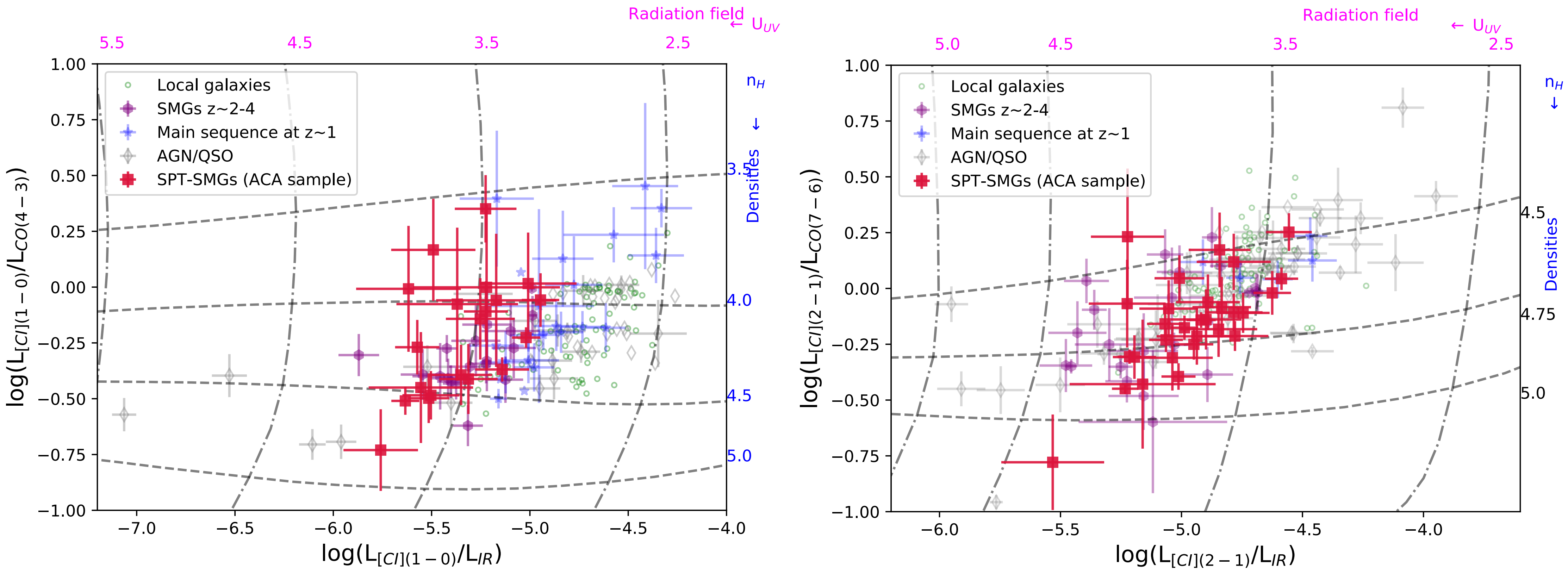

- Comparable radiation field intensities and densities to the SMGs

- Slightly higher radiation field and density compared to the local galaxies despite a small overlap.

Valentino+20 sample

Walter et al. 2011; Alaghband-Zadeh et al. 2013; Bothwell et al. 2017; Yang et al. 2017; Andreani et al. 2018; Cañameras et al. 2018; Nesvadba et al. 2018; Dannerbauer et al. 2019; Jin et al. 2019

Cross-Calibration of gas mass tracers

- We compute the gas mass estimated by [CI](1-0), low-J CO lines, the dust mass and the [CII] line.

- Unknowns : X_{CI}, $\boldsymbol{\alpha}_{CO}$, $\boldsymbol{\delta}_{GDR}$, and $\boldsymbol{\alpha}_{[CII]}$.

- Solution : Cross-calibrate them as a function of all the other known factors.

- We do not provide an absolute calibration which requires to implicitly assume a value for one of these tracers.

$$M(H_2)^{CO} = M(H_2)^{[CI]}$$

$$\Rightarrow \frac{3.39 \times 10^{-2}\, L_{[CI]}}{Q_{10}\, L'_{CO(1-0)}} = X_{CI} \times \alpha_{CO}$$

Cross-Calibration of gas mass tracers

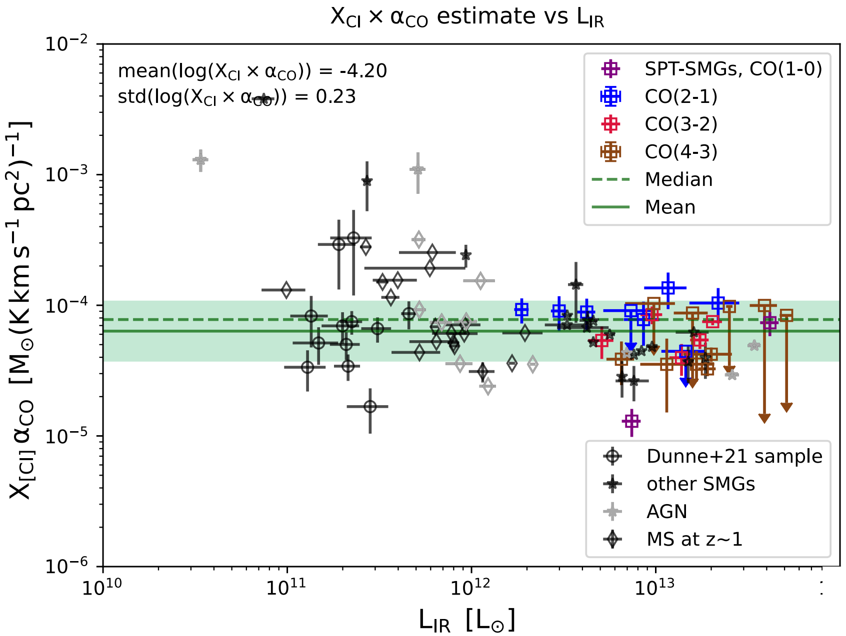

$$M(H_2)^{dust} = M(H_2)^{[CI]}$$

$$\Rightarrow \frac{3.39 \times 10^{-2}\, L_{[CI]}}{Q_{10}\, M_{dust}} = X_{CI} \times \delta_{GDR}$$

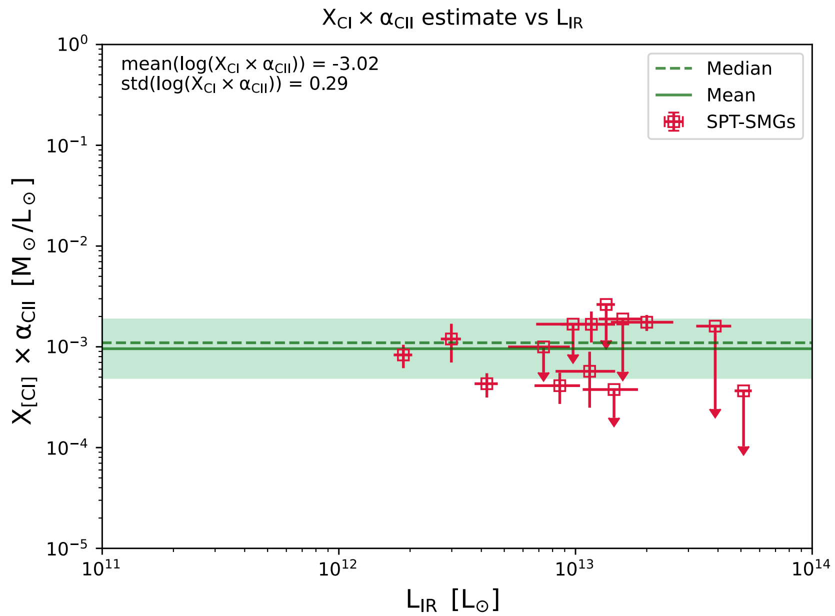

$$M(H_2)^{CO} = M(H_2)^{[CI]}$$

$$\Rightarrow \frac{3.39 \times 10^{-2}\, L_{[CI]}}{Q_{10}\, L'_{CO(1-0)}} = X_{CI} \times \alpha_{CO}$$

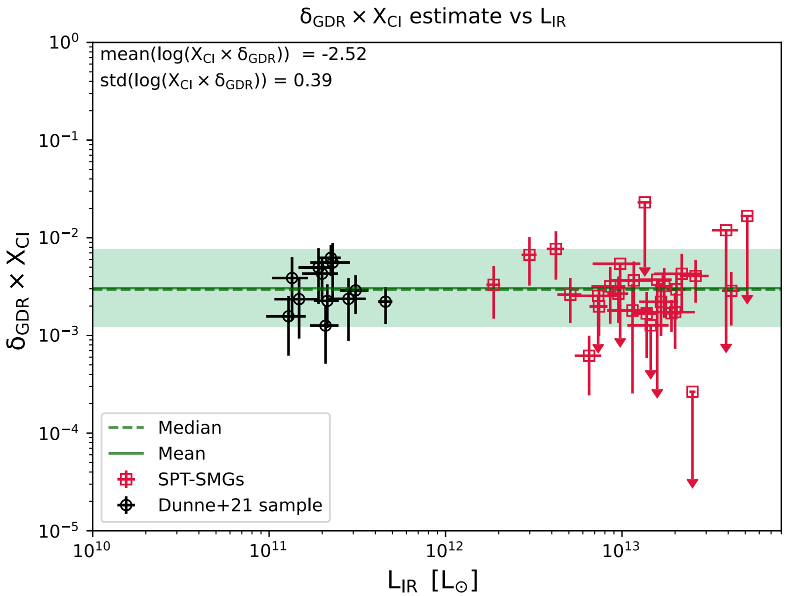

$$M(H_2)^{[CII]} = M(H_2)^{[CI]}$$

$$\Rightarrow \frac{3.39 \times 10^{-2}\, L_{[CI]}}{Q_{10}\, L_{[CII]}} = X_{CI} \times \alpha_{[CII]}$$

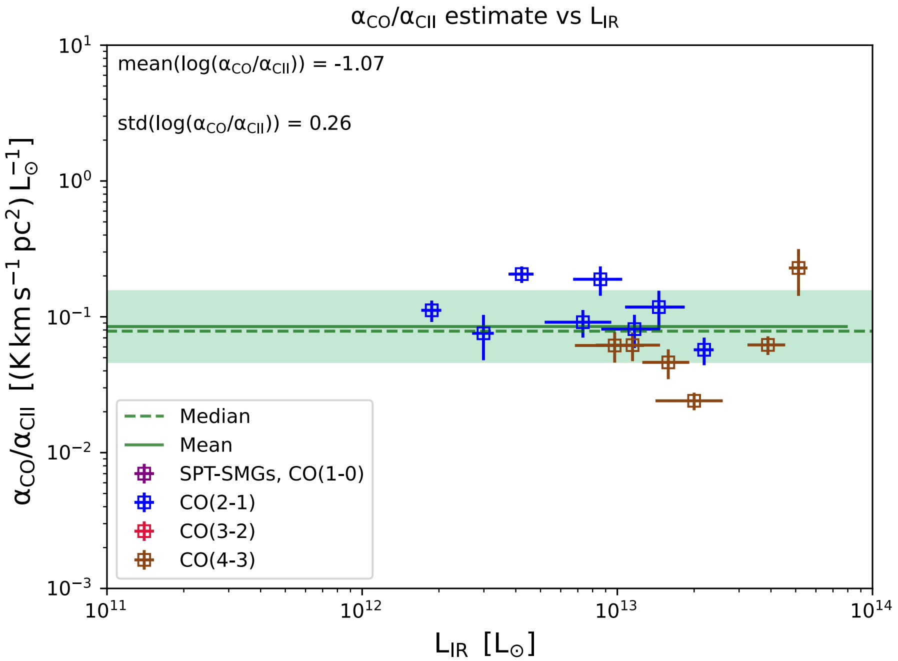

$$M(H_2)^{dust} = M(H_2)^{CO}$$

$$\Rightarrow \frac{L'_{CO(1-0)}}{M_{dust}} = \frac{\delta_{GDR}}{\alpha_{CO}}$$

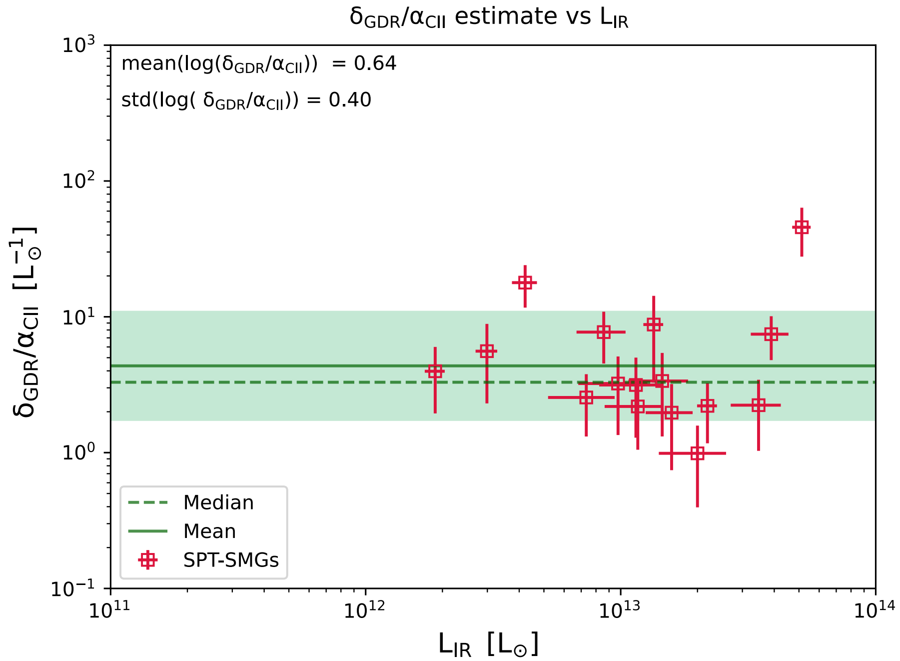

$$M(H_2)^{[CII]} = M(H_2)^{CO}$$

$$\Rightarrow \frac{L_{[CII]}}{L'_{CO(1-0)}} = \frac{\alpha_{CO}}{\alpha_{[CII]}}$$

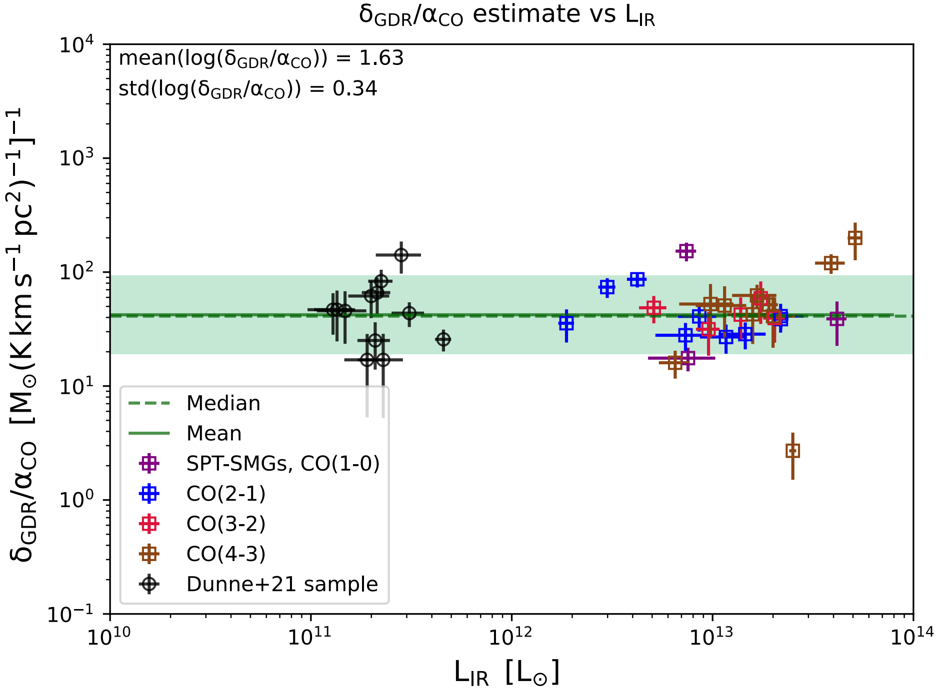

$$M(H_2)^{dust} = M(H_2)^{[CII]}$$

$$\Rightarrow \frac{L_{[CII]}}{M_{dust}} = \frac{\delta_{GDR}}{\alpha_{[CII]}}$$

Conclusions on the cross-calibrations

- Tracers agree reasonably well!
- Significant fraction of the scatter can be modelled by measurement uncertainties.
- No strong trend with L_{IR}.
- Assuming $\boldsymbol{\alpha}_{CO}$ ~3.4 (Jarugula+21) ⇒ X_{CI} ~ 1.86±0.20*10^{-5} $\boldsymbol{\delta}_{GDR}$ ~ 145±22, and $\boldsymbol{\alpha}_{[CII]}$ ~ 40±6 $M_{\odot}/L_{\odot}$.
- Assuming $\boldsymbol{\alpha}_{CO}$ ~0.8 (Downes & Solomon 98, Engel+10, ULIRG like value) ⇒ X_{CI} ~ 7.9±0.8*10^{-5} , $\boldsymbol{\delta}_{GDR}$ ~ 34±5 (possible in metal rich environments, Litke+23, De Breuk+19) and $\boldsymbol{\alpha}_{[CII]}$ ~ 9.4±1.5 $M_{\odot}/L_{\odot}$.

Cross-calibration of tracers	Value
$X_{CI} \times \alpha_{CO}$ $(\times 10^{-5})$	6.31±0.67
$X_{CI} \times \alpha_{[CII]}$ $(\times 10^{-5})$	95.5 ±17.1
$X_{CI} \times \delta_{GDR}$ $(\times 10^{-5})$	302.0±52.2
$\alpha_{CO}/\alpha_{[CII]}$	0.08±0.01
δ_{GDR}/α_{CO}	42.66 ±6.43
$\delta_{GDR}/\alpha_{[CII]}$	4.36±1.07

Depletion timescales of the sample

- Using the CO-estimated gas mass, we compute the depletion timescales of these galaxies with two values of $\boldsymbol{\alpha}_{\mathrm{CO}}$.
- Higher $\boldsymbol{\alpha}_{\mathrm{CO}}$ (~3.4) gives longer depletion timescales, indicating the population to be in the main-sequence.
- Lower $\boldsymbol{\alpha}_{\mathrm{CO}}$ (~0.8) gives shorter depletion times, which is suggestive of a starburst-like population.

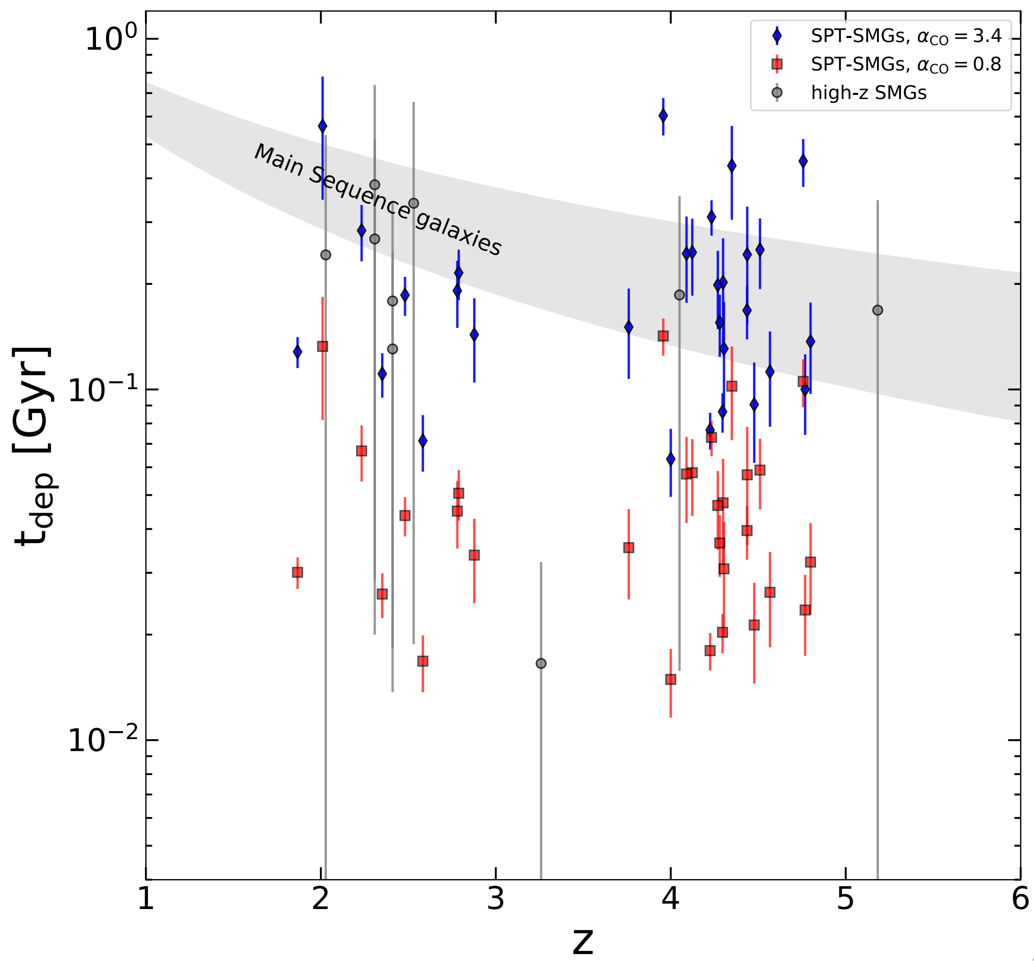

Insights on the nature of these DSFGs from high-resolution (~0.3”) imaging with ALMA

Gururajan+22,
10.1051/0004-6361/202142172

Sample

Resolution ~ 0.3”; Observed : [CI](2-1), CO(7-6) and continuum emission

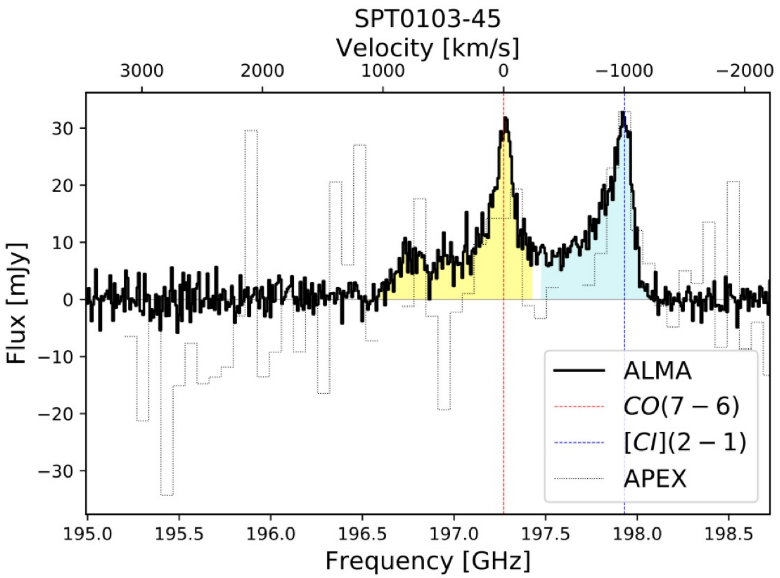

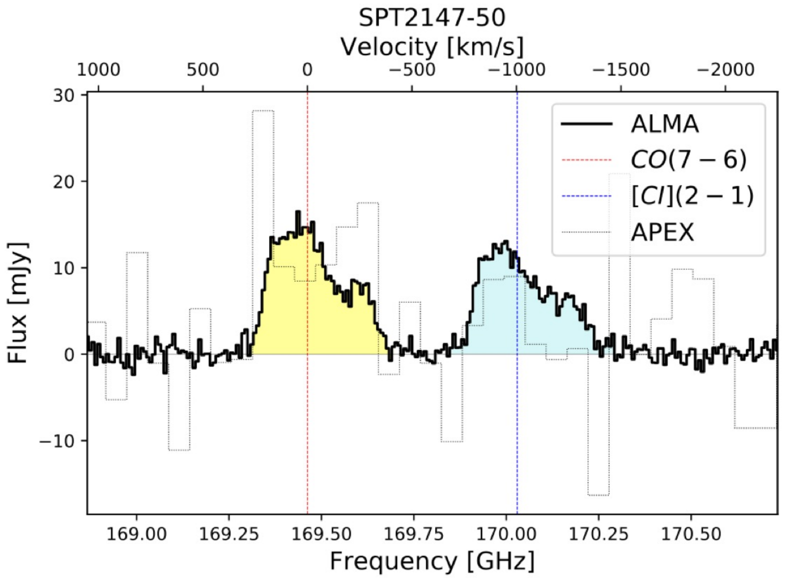

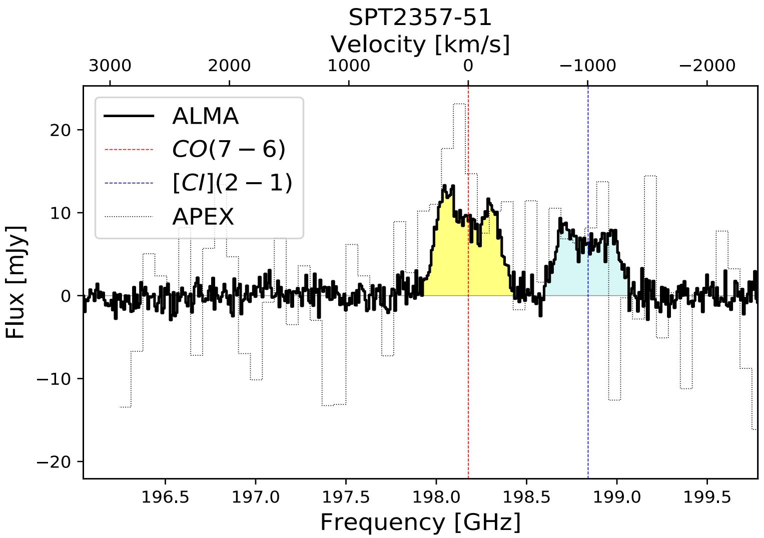

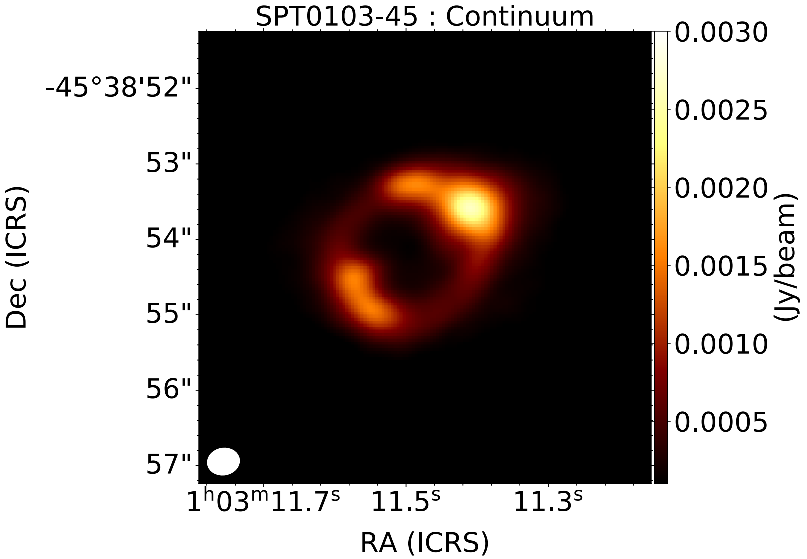

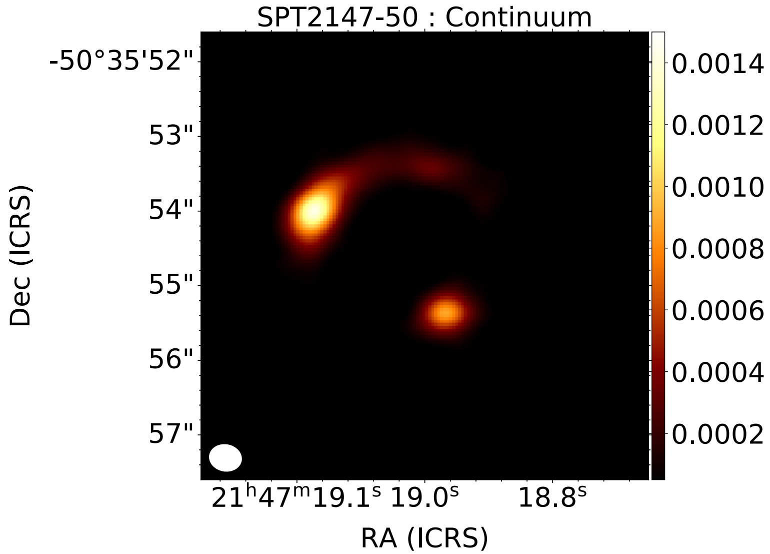

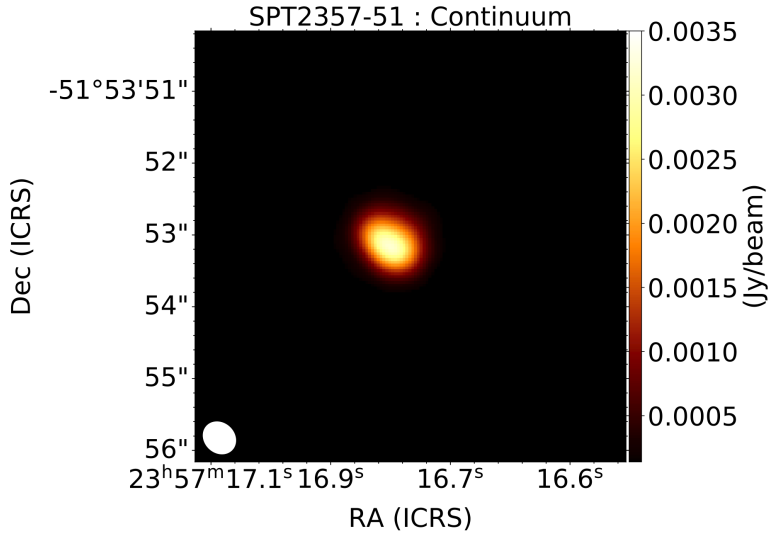

Image plane kinematics

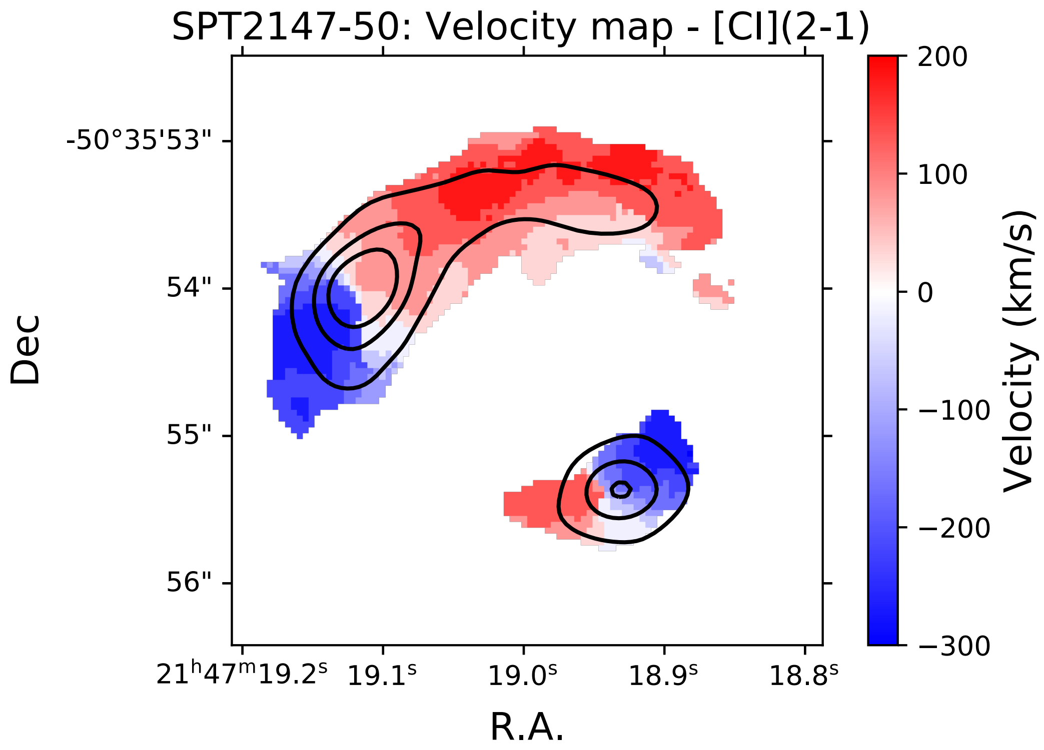

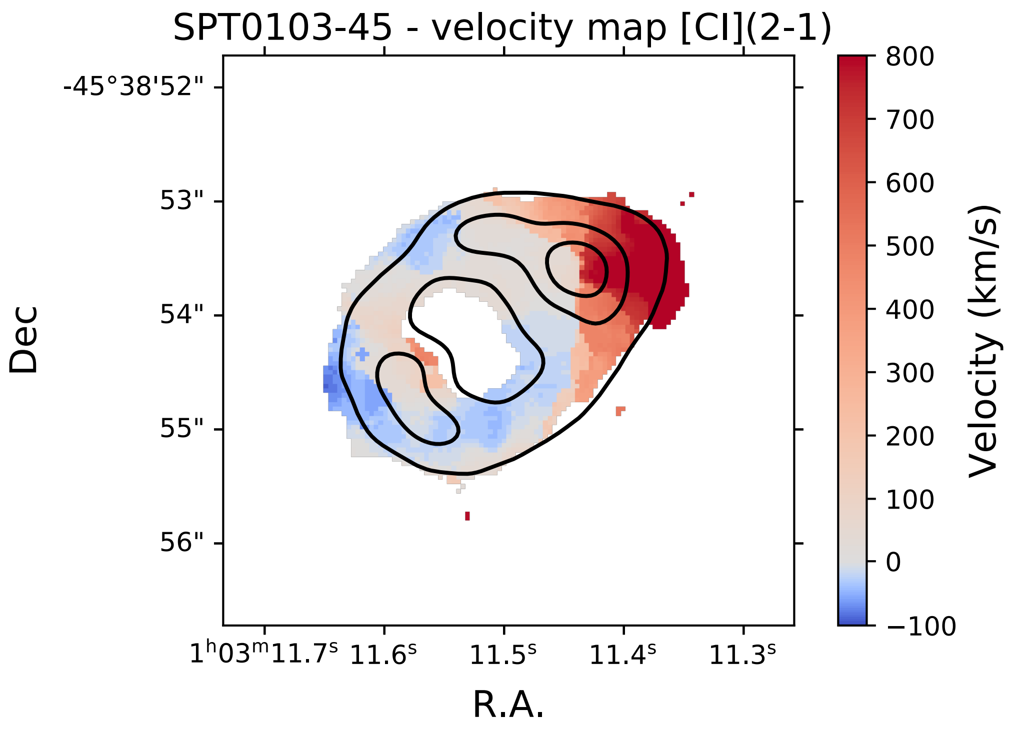

- Pixel-wise velocity maps – Identify peak of emission and the corresponding velocity at every line-of-sight.
- The velocity maps of both the sources show a smooth gradient which could be suggestive of their rotation.
- SPT0103-45 and SPT2147-50 : Probable rotators

Image plane kinematics

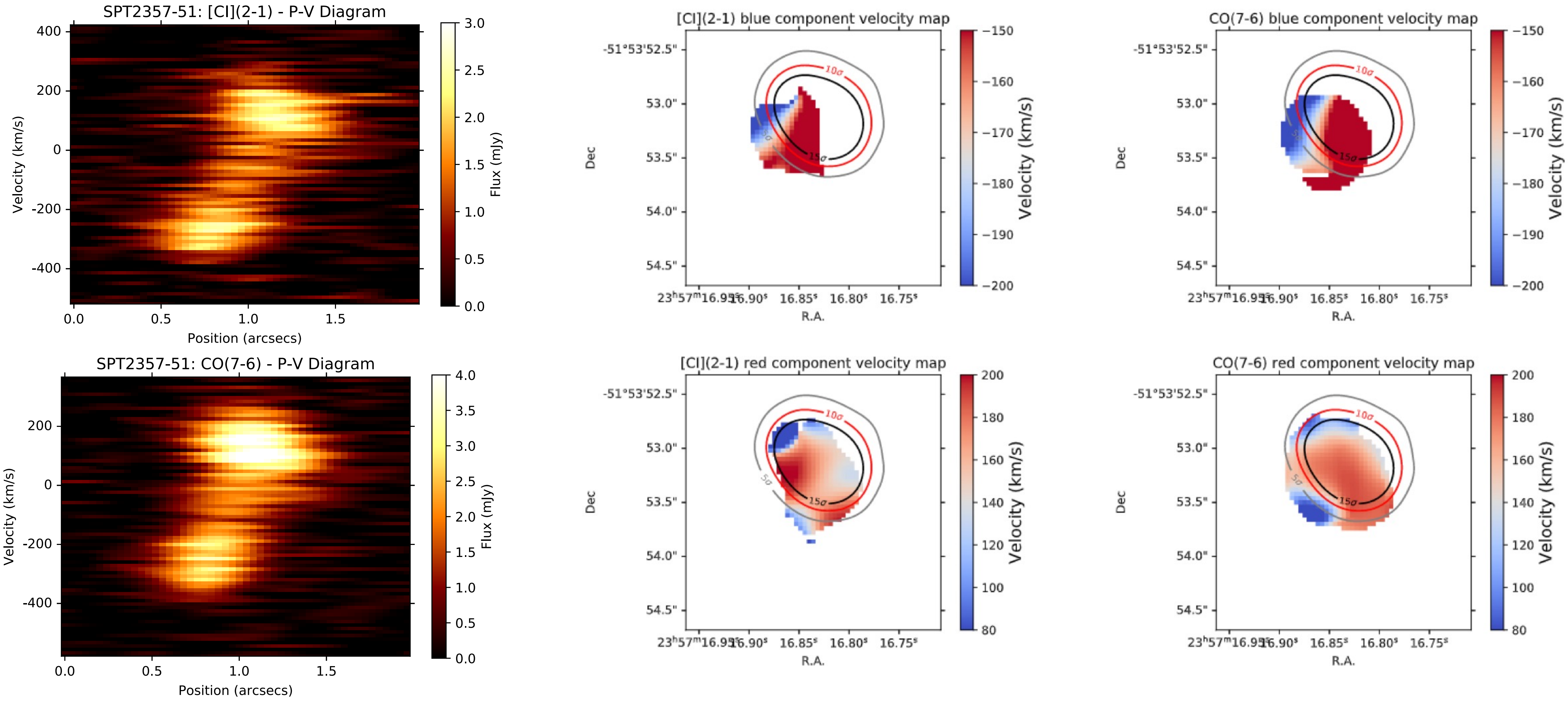

- Position-velocity diagram : Two components which seem to be connected by a bridge like structure
- Pixel-wise decomposition of the spectra using a double-Gaussian profile for the lines.
- SPT2357-51 : Possible merger candidate

Lens modelling

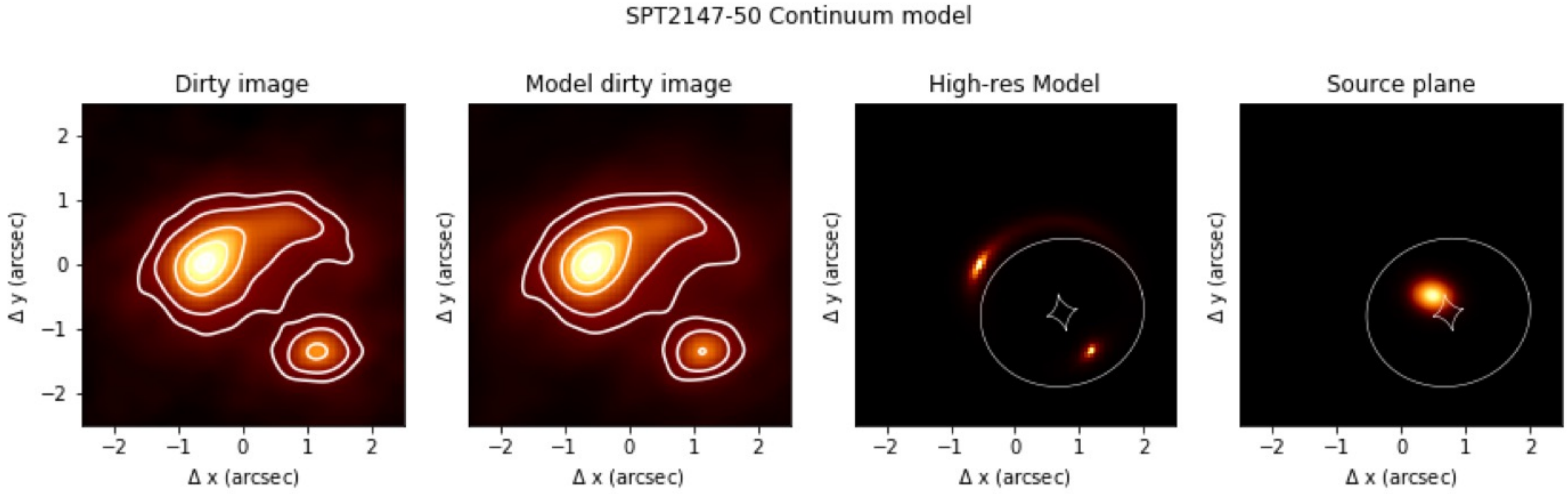

Modelling the lensing configuration with visibility-based modelling code visilens (Spilker+16).

Source-plane Kinematics

To model the source-plane velocity, we plot the positions from the lens modeling of the line emissions for every velocity bin.

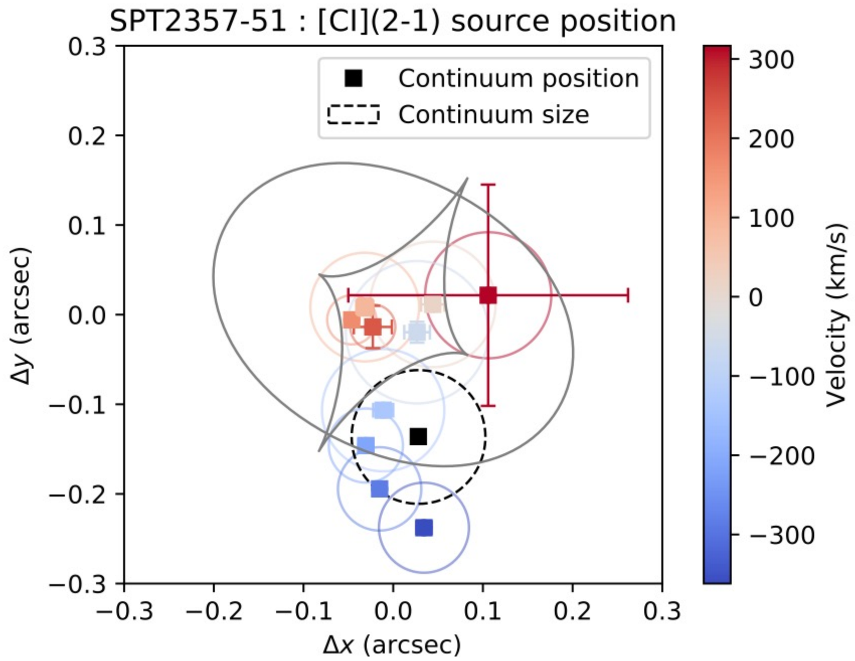

SPT2357-51 : Possible merging system

SPT0103-45 and SPT2357-51 : Probable rotators.

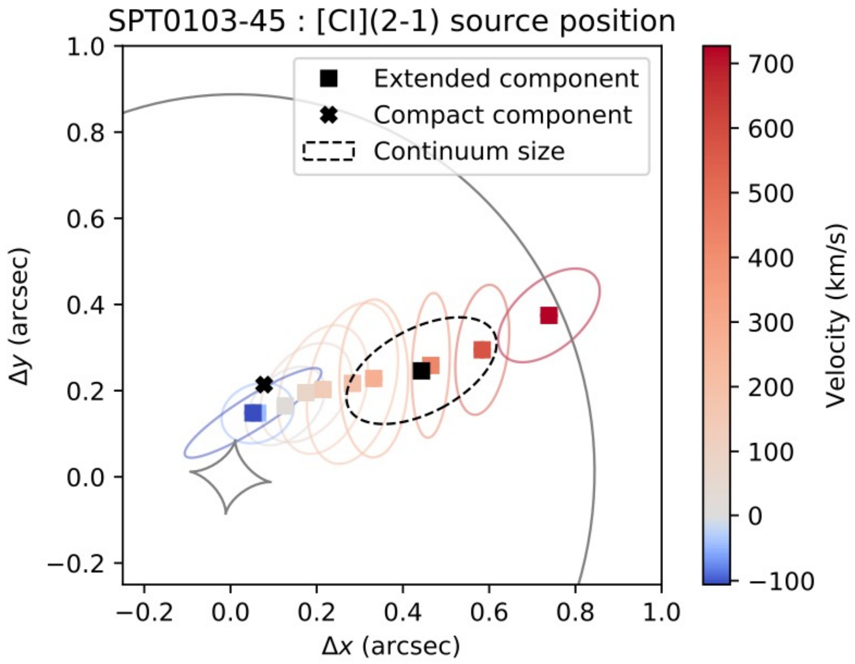

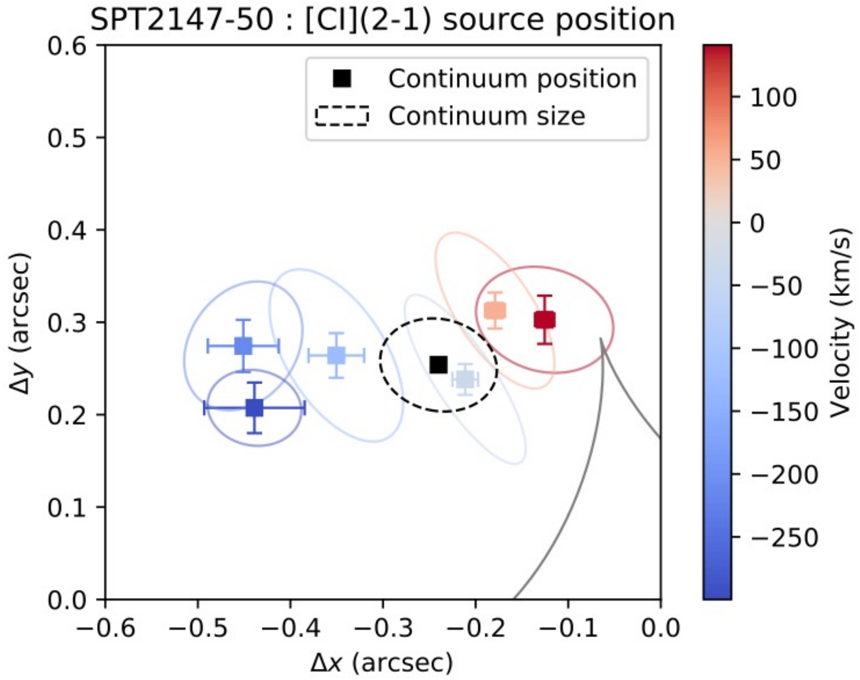

Differential magnification

- Differential magnification : comparing the effective magnification of the lines to the continuum magnification.
- The asymmetries observed in the line profiles of SPT0103-45 and SPT2147-50 directly linked to magnification effects.
- However, no strong effect (<24%) is seen on the total fluxes

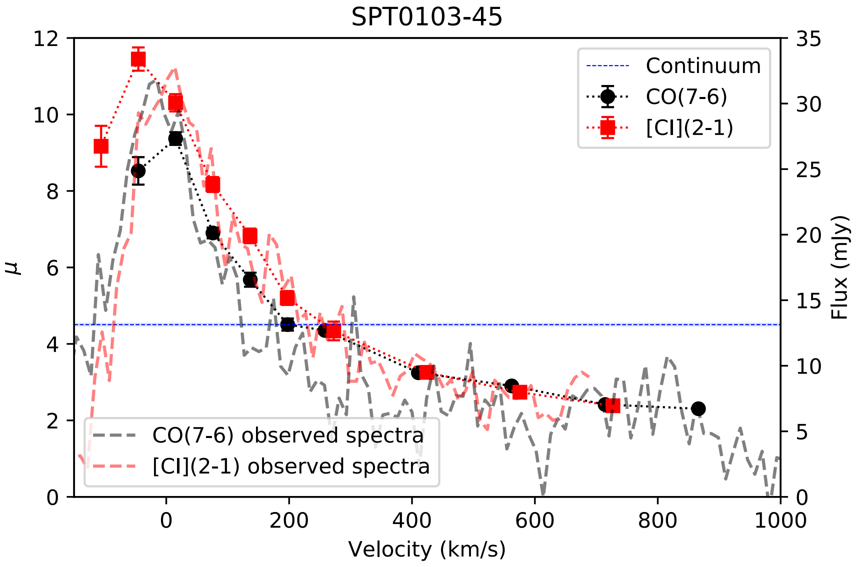

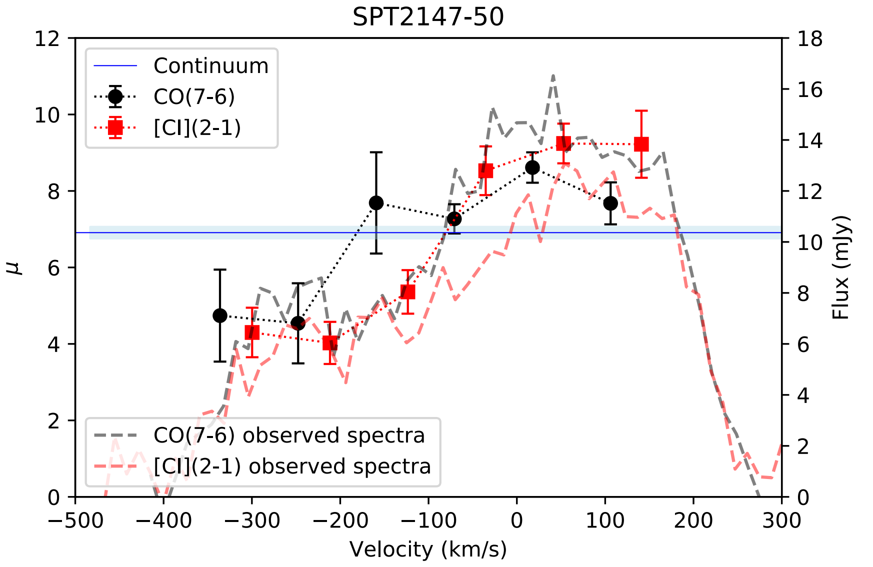

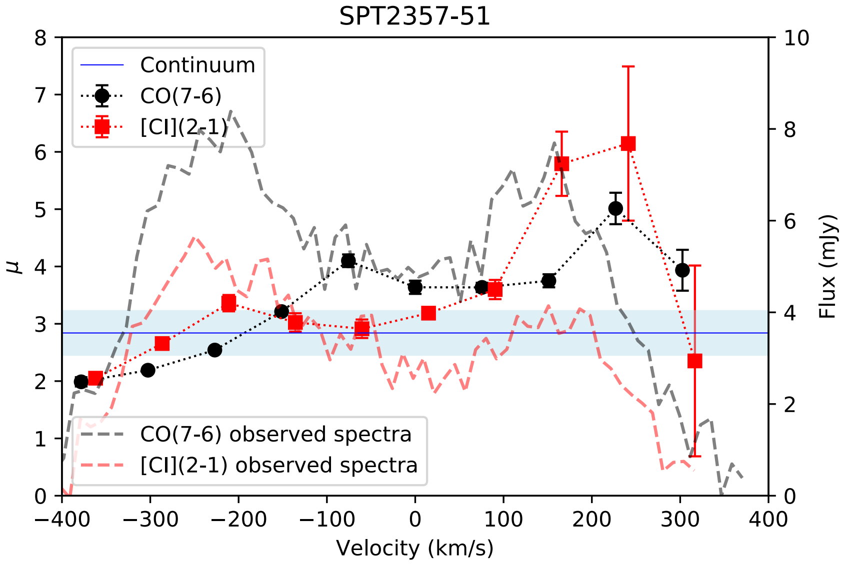

Source	μ_{eff} [CI](2-1)	μ_{eff} CO(7-6)	μ Continuum
SPT0103-45	6.2±0.2	5.6±0.1	4.7±0.6
SPT2147-50	6.7±0.3	6.9±0.4	6.9±0.2
SPT2357-51	3.1±0.2	3.3±0.1	2.8±0.4

Resolved ISM diagnostics using line ratios

- Our sample have comparable radiation field intensities and densities to the SMGs and main sequence galaxies at z~1.

- The ISM of our sources (pixels in the figure) exhibit a heterogeneity, showing variations in the radiation field and density across the source.

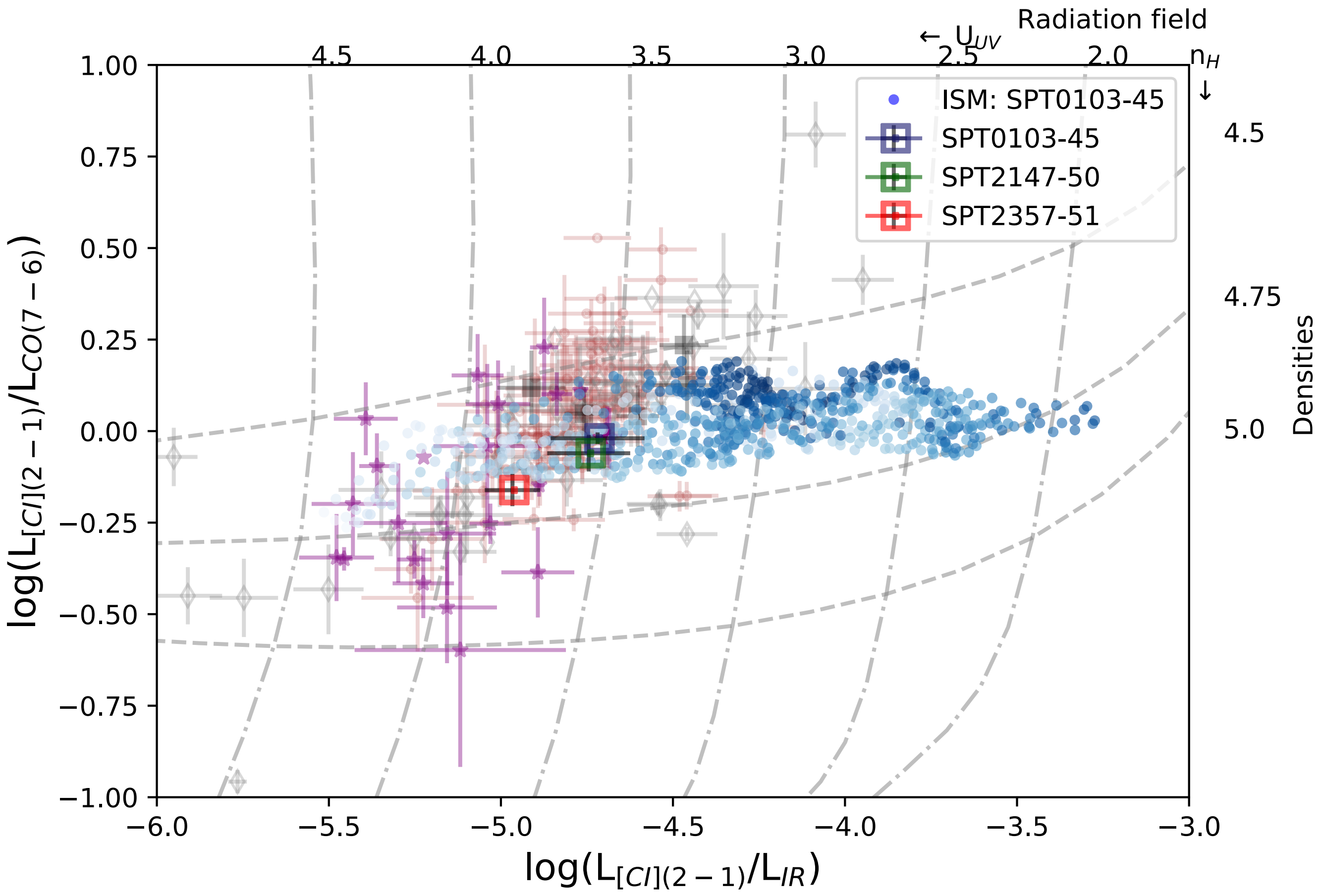

Valentino+20 sample
Walter et al. 2011; Alaghband-Zadeh et al. 2013; Bothwell et al. 2017; Yang et al. 2017; Andreani et al. 2018; Cañameras et al. 2018; Nesvadba et al. 2018; Dannerbauer et al. 2019; Jin et al. 2019

Understanding the depletion timescales of our sample

- Computing the dynamical masses of the two rotators using a simple Keplerian approach.
- Gas mass estimated with α_{CO} = 0.8 was agreeable with the dynamical mass, a higher α_{CO} = 3.4 was in tension with the dynamical mass.
- With α_{CO} = 0.8, our sample have a short depletion time scale < 100 Myr.
- However, we are limited by a very small sample.

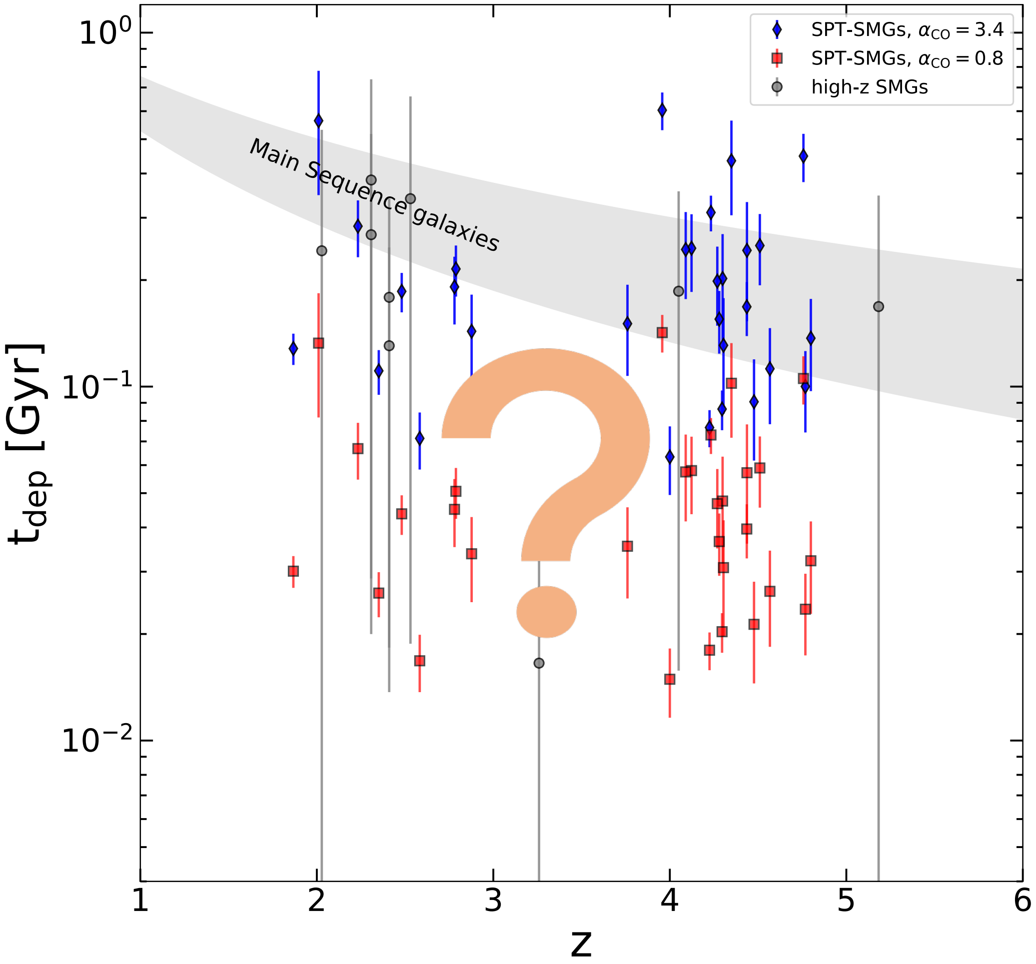

Conclusions

Nature of massive, intensely star-forming high-z DSFGs

Gas Content

- Three tracers : CO, [CI], [CII] and dust – each with their uncertainties.
- $\boldsymbol{\alpha}_{CO}$, X_{CI} , $\boldsymbol{\alpha}_{CII}$ and $\boldsymbol{\delta}_{GDR}$: Cross calibrated for our sample.
- The four tracers have a good agreement with each other.
- No strong trend with L_{IR}.

ISM properties

- Similar U_{UV} and n_H to SMGs, but higher than the local galaxies.
- Heterogeneity in the U_{UV} and n_H across the ISM.
- CI-excitation temperatures are comparable to the SMGs.
- T_{ex} lower than T_{dust} for our sample.

Morpho-kinematics

Morpho-kinematic diversity in our high-resolution analysis : rotating-starbursting disks to merging systems.

Differential magnification

- Line fluxes are not significantly affected by differential magnification.
- Line profiles are strongly affected by magnification effectes.

Thank you

Gururajan+23

Gururajan+22

Backup!!!!!

L_{IR} versus $L_{[CI]}$

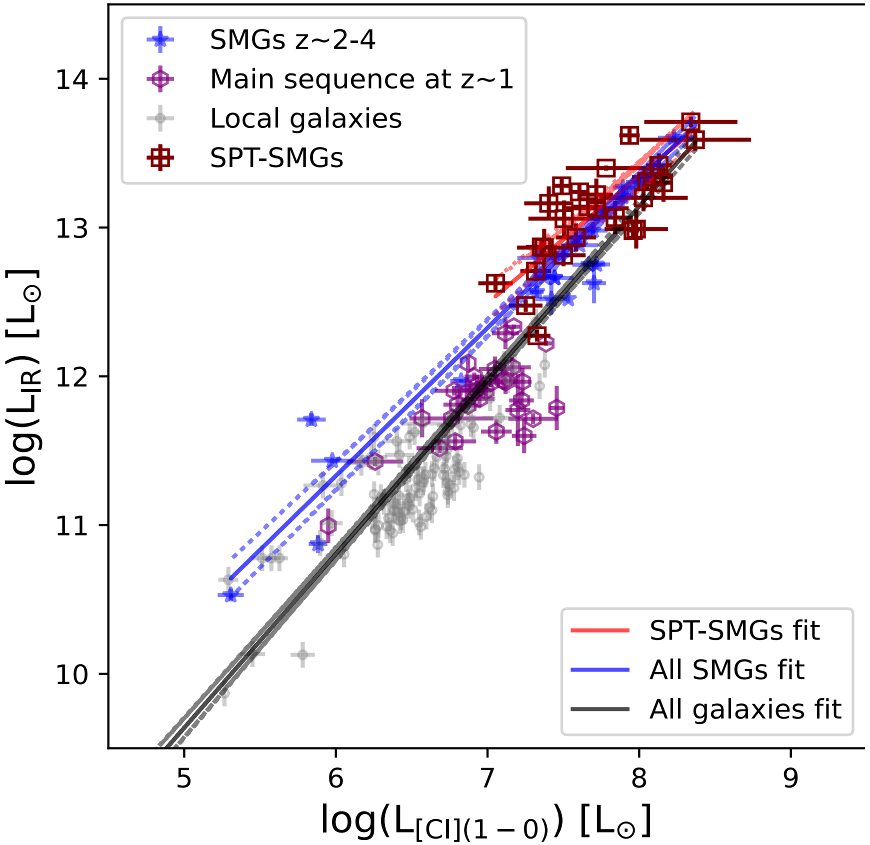

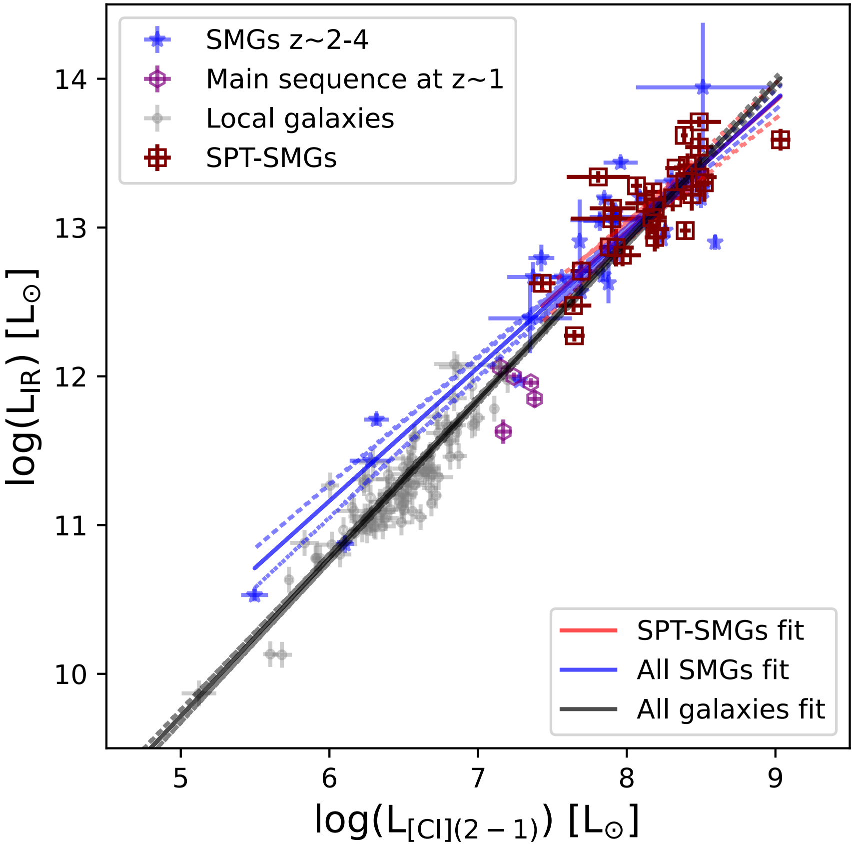

- [CI] : gas tracer and IR :SFR tracer [CI]-L_{IR} relation: integrated KS relation
- [CI](1-0) vs L_{IR} : SMGs and local galaxies have a nearly linear slope, but the slope is super-linear for a combined sample (different trend for MS and Starbursts? Daddi+10, Genzel+10).
- [CI](2-1) vs L_{IR} : Slope is nearly linear across all populations, (higher excitation of [CI](2-1) in starbursts could be a factor).

Sample	Slope (β) [CI](1-0) dex	Intercept (α) [CI](1-0) dex	Slope (β) [CI](2-1) dex	Intercept (α) [CI](2-1) dex
SPT-SMGs	0.90±0.17	6.14±1.28	0.88±0.14	5.94±1.11
All SMGs	1.00±0.05	5.34±0.41	0.90±0.05	5.77±0.42
Local galaxies and main-sequence at $z \sim 1$	0.98±0.04	4.95±0.23	1.02±0.03	4.63±0.19
Full sample	1.16±0.03	3.83±0.21	1.06±0.02	4.40±0.13

Excitation temperature of [CI]

- Most of our sources have larger dust temperatures than the [CI]-excitation temperature.

- Plausible explanation : The dusty cores of these galaxies are warmed by the intense star formation, whereas the [CI] trace more extended, less dense regions.

- Our results does not favor optically thick dust scenario (GN20 – Cortzen+20).

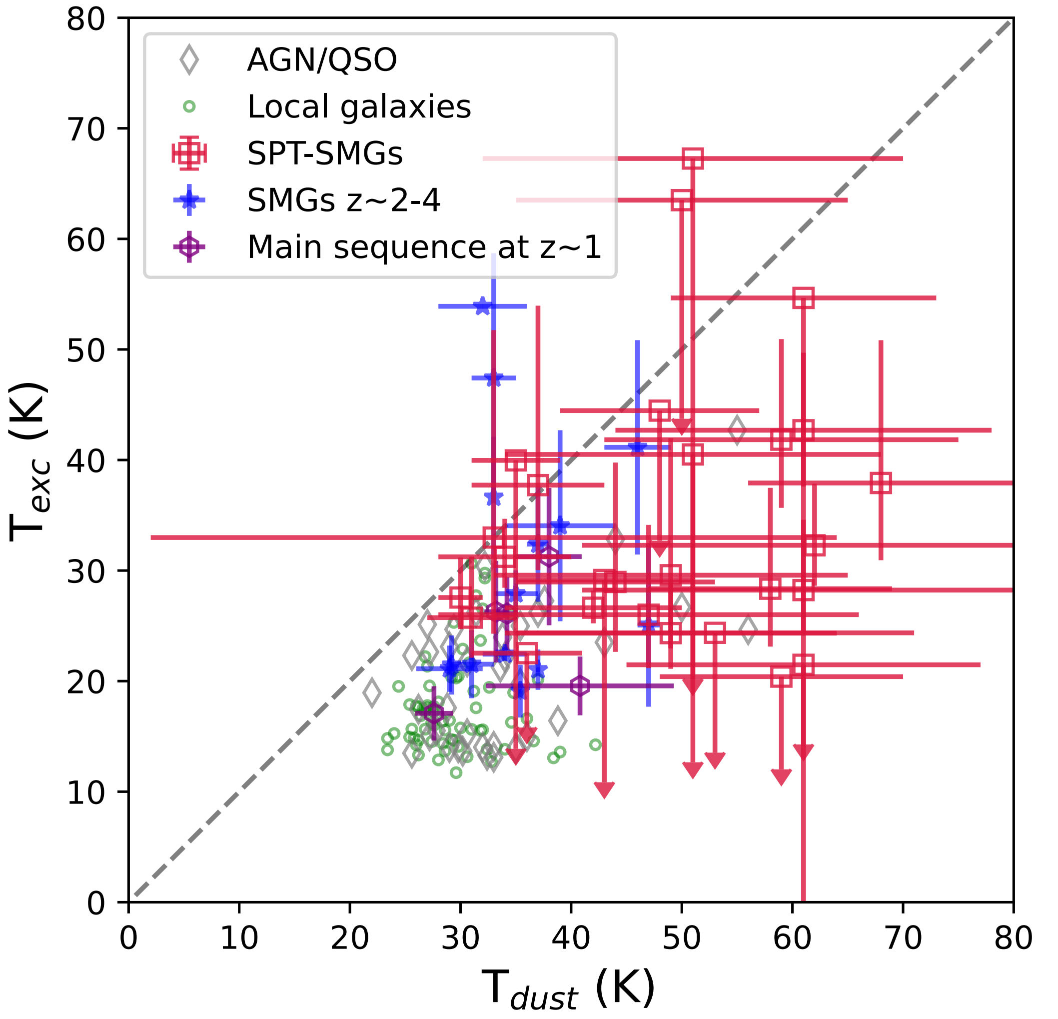

[CI]-excitation fraction – Q_{10}

- With the two [CI] line fluxes, we can constrain the [CI] excitation fraction.
- We use the following formula

$$Q_{10} = 3e^{-T1/Tex} / 1 + 3e^{-T1/Tex} + 5e^{-T2/Tex},$$

where, T_1 = 23.6 K and T_2 = 62.5 K which are the two excitation levels of neutral carbon.

- Median Q_{10} of the sample : 0.45 ± 0.01.

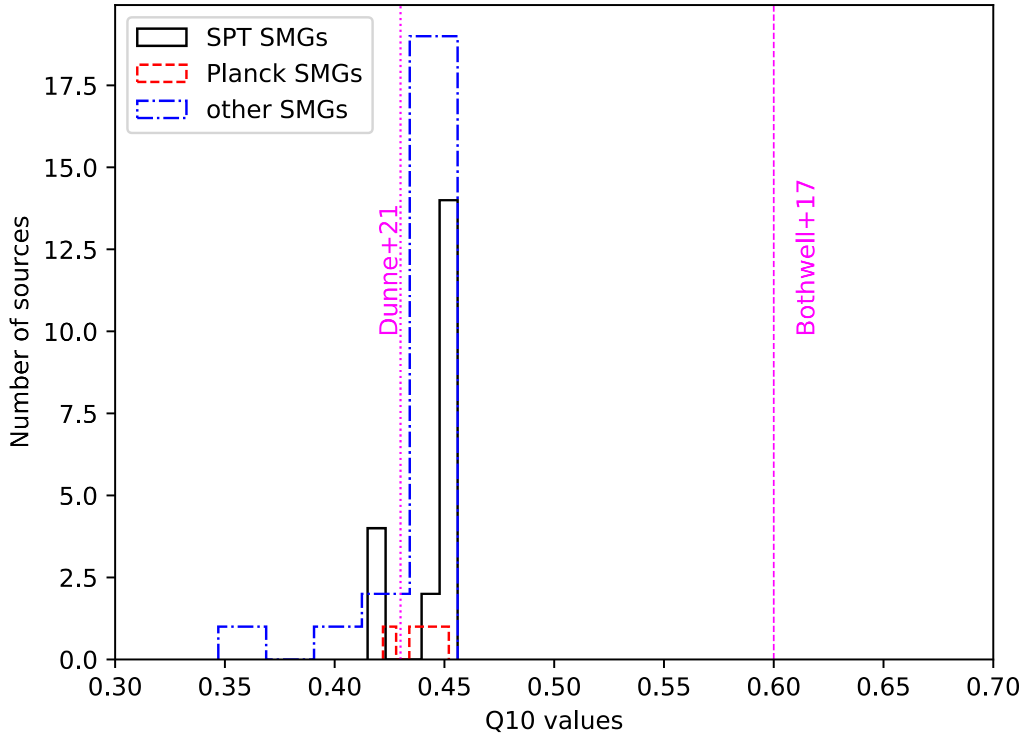

Is the scatter driven by the measurement uncertainties?

- We perform the following test to determine this. Consider the case of XCI*alphaCO plot.

- Assuming the median value, we generate mock L'CO values using a random gaussian generator.

$$\frac{1375.8\ D_L^2\ S_\nu \Delta v}{(1+z)\ Q_{10}\ A_{10}\ median(X_{CI} \times \alpha_{CO})} = L'_{CO}$$

- We recompute the XCI*alphaCO using the mock L'CO values and compare it with our data.

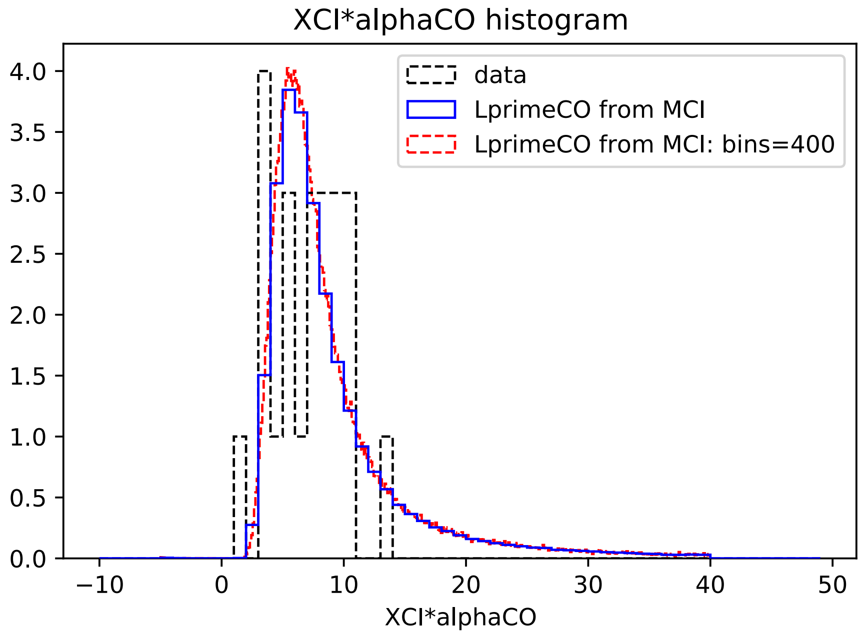

stddev of log(data): 0.2232
stddev of log(LpCO from MCI/median): 0.2198

KstestResult(statistic=0.1805771890986143, pvalue=0.39415746390053674)

Scatter and ks test

Table D.1. KS test between the observed data and the simulated data with noise

Data	Deviation	p-Value
$X_{CI} \times \alpha_{CO}$	0.18	0.39
$X_{CI} \times \alpha_{[CII]}$	0.30	0.13
$X_{CI} \times \delta_{GDR}$	0.18	0.35
$\alpha_{CO} / \alpha_{[CII]}$	0.21	0.48
$\delta_{GDR} / \alpha_{CO}$	0.15	0.50
$\delta_{GDR} / \alpha_{[CII]}$	0.32	0.06

Dust temperature versus gas tracers

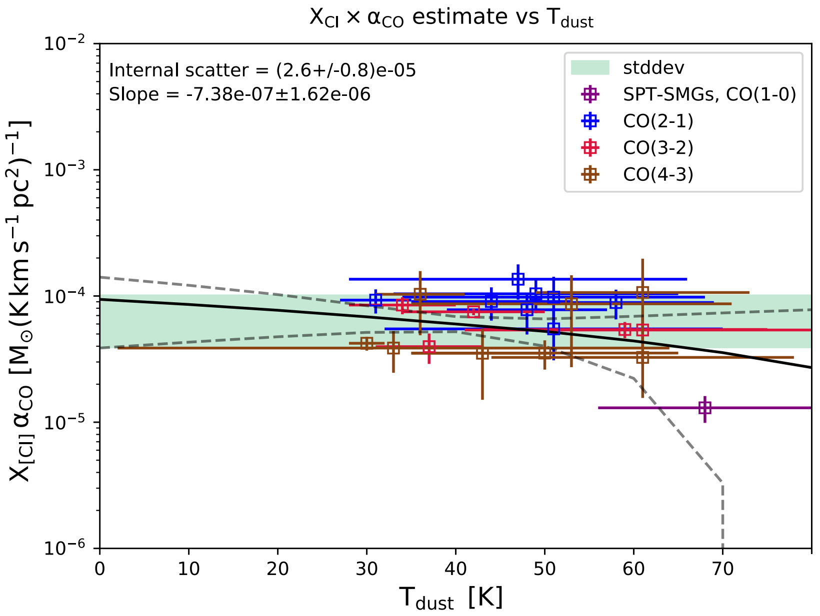

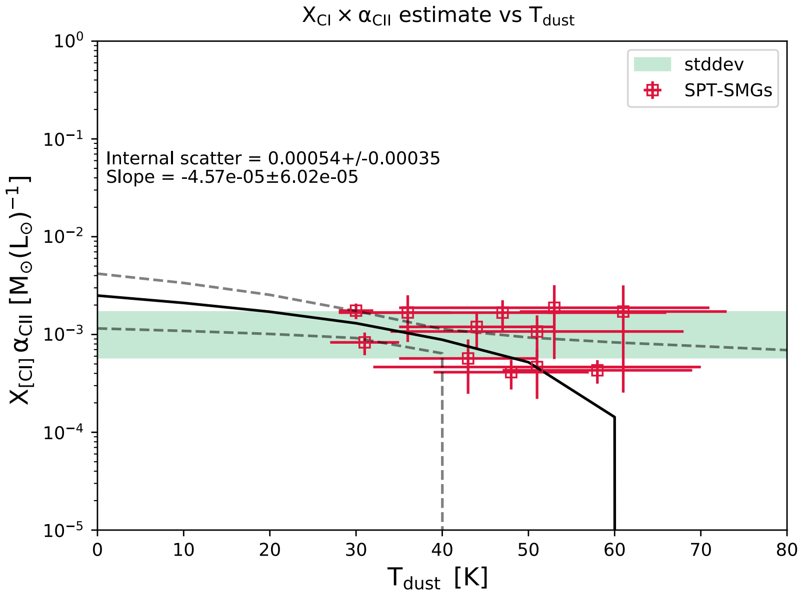

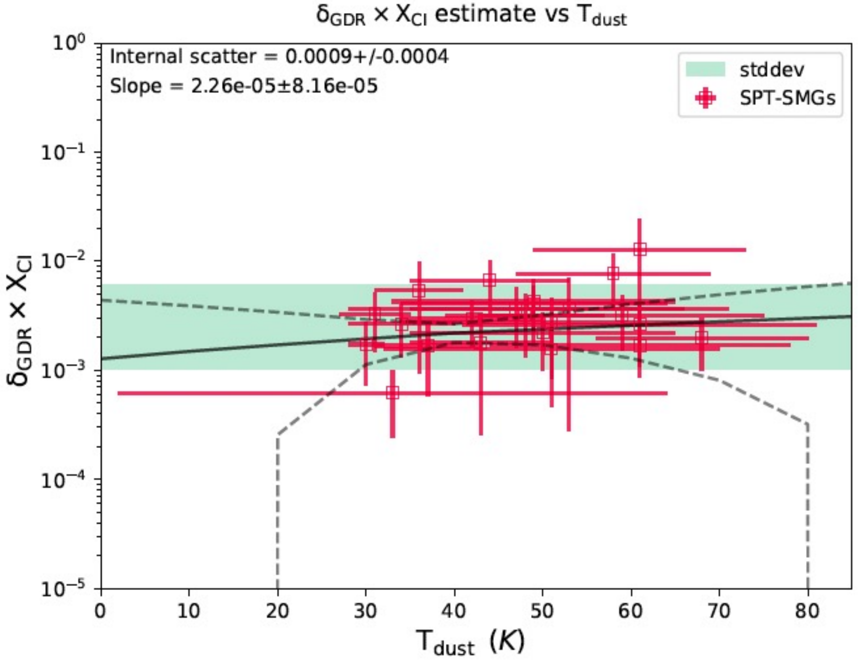

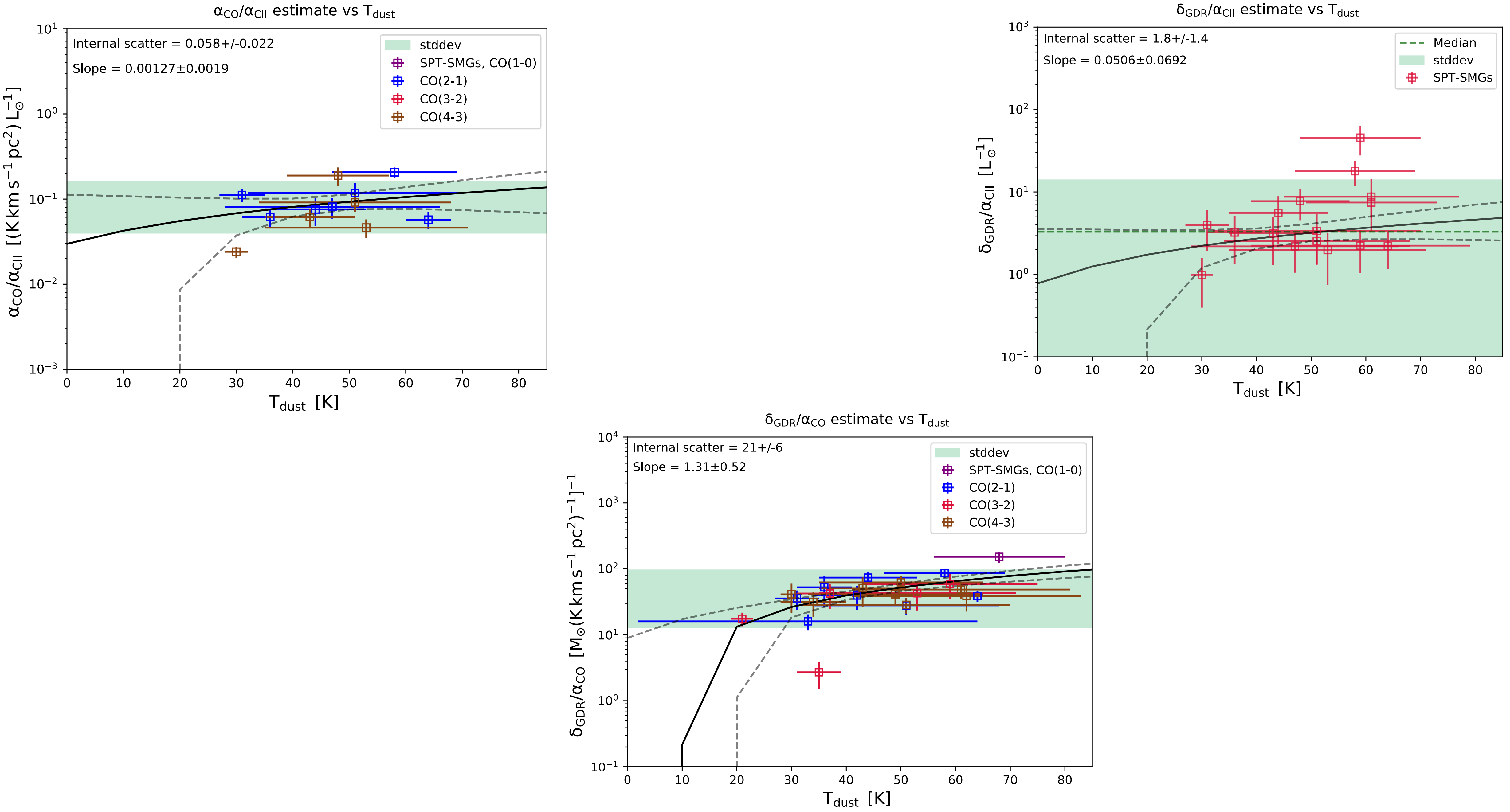

α_{CO}/α_{CII} estimate vs T_{dust}
Internal scatter = 0.058+/-0.022
Slope = 0.00127±0.0019
stddev
SPT-SMGs, CO(1-0)
CO(2-1)
CO(3-2)
CO(4-3)
α_{CO}/α_{CII} [(K km s^{-1} pc^2) $L_\odot^{-1}$]
T_{dust} [K]
$\delta_{GDR}/\alpha_{CII}$ estimate vs T_{dust}
Internal scatter = 1.8+/-1.4
Slope = 0.0506±0.0692
Median
stddev
SPT-SMGs
$\delta_{GDR}/\alpha_{CII}$ [$L_\odot^{-1}$]
T_{dust} [K]
δ_{GDR}/α_{CO} estimate vs T_{dust}
Internal scatter = 21+/-6
Slope = 1.31±0.52
stddev
SPT-SMGs, CO(1-0)
CO(2-1)
CO(3-2)
CO(4-3)
δ_{GDR}/α_{CO} [$M_\odot$(K km s^{-1} pc^2)$^{-1}$]$^{-1}$
T_{dust} [K]

SPT0103-45

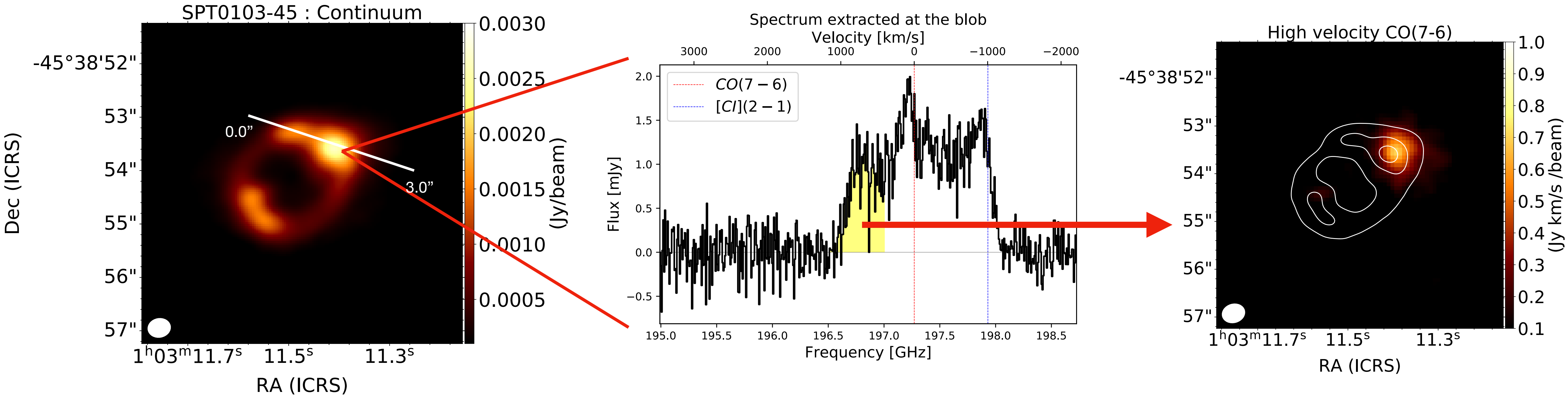

Two most intriguing features : gem and the unidirectional, high-velocity tail.

Position-velocity diagram

SPT2357-51

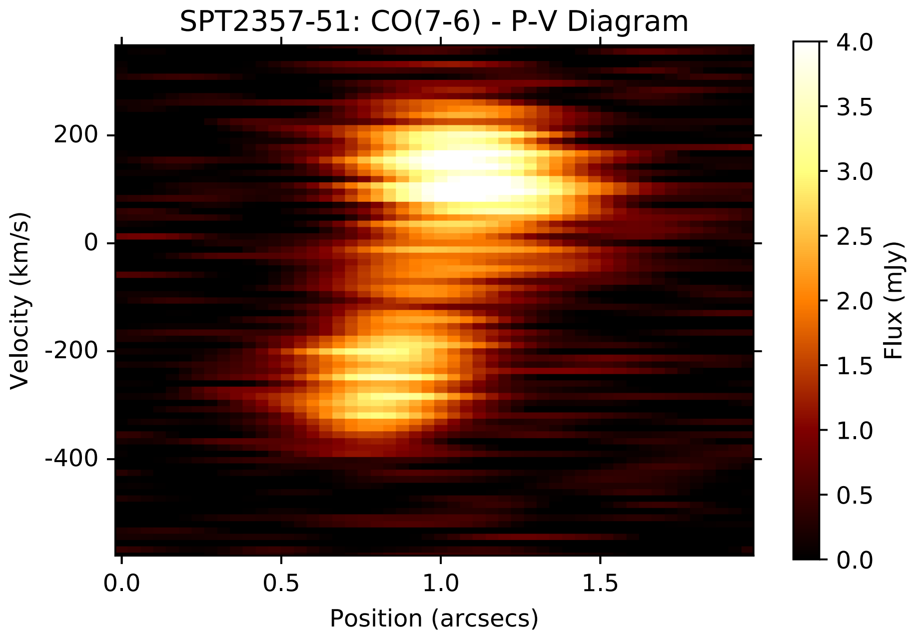

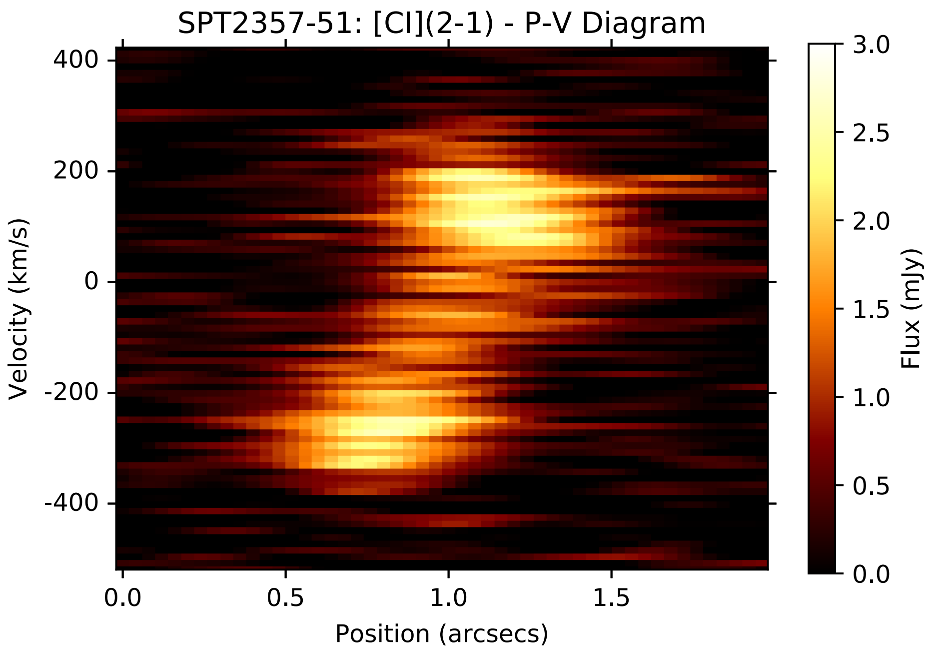

- Position velocity diagram of a slice along the RA axis of the source
- Two components which seem to be connected by a bridge like structure
- Maybe a merging scenario?

Gaussian decomposition of the spectra

- SPT2357-51 : double peak profile for both the lines in its integrated spectra.

- Pixel-wise decomposition of the spectra using a double-Gaussian profile for the lines.

- Example of the fit for a single line of sight.

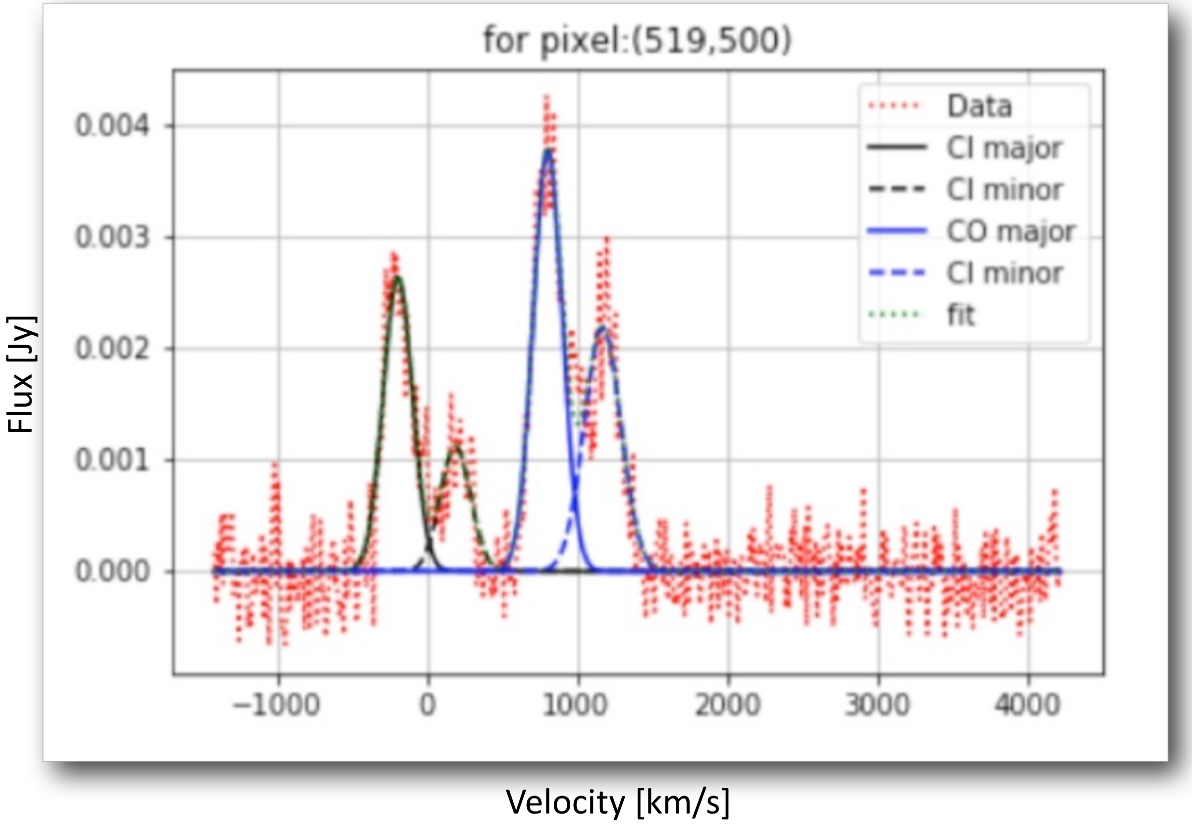

Position-velocity diagram

- Extracted a slice along the arc.
- CO(7-6) reference velocity set as zero-velocity.

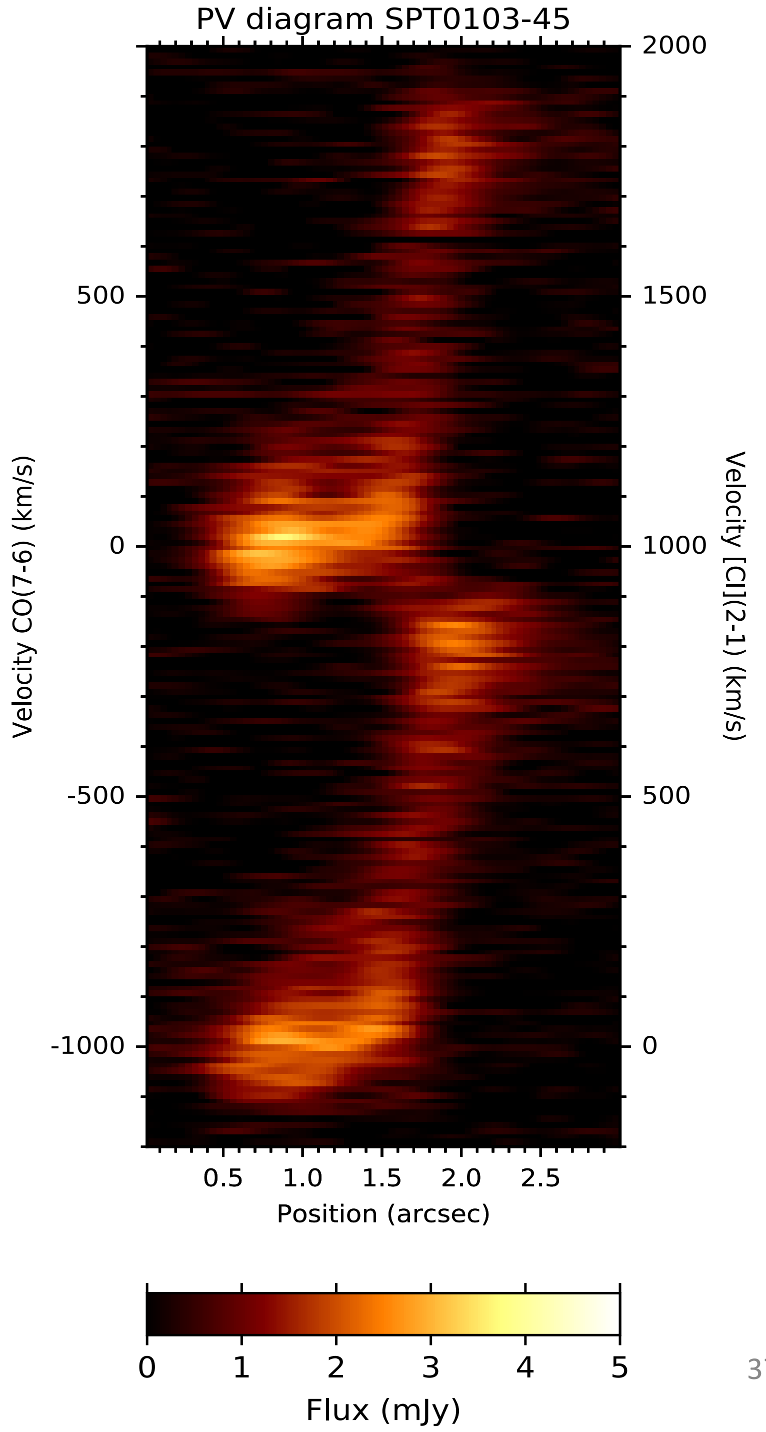

Results

- Our sources have a high intrinsic SFR > 800 $M_\odot$ / yr. We estimated the gas mass of our sample with ancillary CO(3-2) data and [CI](1-0) for SPT2147-50.

- From the source size estimates and axis ratios, we compute the dynamical mass using a simple Keplerian approach.

- Gas mass estimated with α_{CO} = 0.8 was agreeable with the dynamical mass, a higher α_{CO} = 3.4 was in tension with the dynamical mass.

- With these gas mass (α_{CO} = 0.8), we can also calculate the depletion time scales. Our sample have a short depletion time scale < 100 Myr.

$$M_{dyn} = \frac{R V_{obs}^2}{G \sin^2(i)}$$

Radius estimated from the velocity modelling

Projected component of the velocity

cos(i) = b/a;
i.e. axis ratio